

1 Remotely sensed soil moisture can capture dynamics relevant to plant water uptake

2

3 Andrew F. Feldman^{1,2}, Daniel J. Short Gianotti³, Jianzhi Dong³, Ruzbeh Akbar³, Wade
4 T. Crow⁴, Kaighin A. McColl^{5,6}, Alexandra G. Konings⁷, Jesse B. Nippert⁸, Shersingh
5 Joseph Tumber-Dávila⁹, Noel M. Holbrook¹⁰, Fulton E. Rockwell¹⁰, Russell L. Scott¹¹,
6 Rolf H. Reichle¹², Abhishek Chatterjee¹³, Joanna Joiner¹⁴, Benjamin Poulter¹, Dara
7 Entekhabi³

8

9 ¹Biospheric Sciences Laboratory, NASA Goddard Space Flight Center, Greenbelt, MD,
10 USA

11 ²NASA Postdoctoral Program, NASA Goddard Space Flight Center, Greenbelt, MD,
12 USA

13 ³Department of Civil and Environmental Engineering, Massachusetts Institute of
14 Technology, Cambridge, Massachusetts, USA

15 ⁴USDA ARS Hydrology and Remote Sensing Laboratory, Beltsville, Maryland, USA

16 ⁵Department of Earth and Planetary Sciences, Harvard University, Cambridge, MA, USA

17 ⁶Harvard John A. Paulson School of Engineering and Applied Sciences, Harvard
18 University, Cambridge, MA, USA

19 ⁷Department of Earth System Science, Stanford University, Stanford, California, USA

20 ⁸Division of Biology, Kansas State University, Manhattan, KS, USA

21 ⁹Harvard Forest, Harvard University, Petersham, MA, USA

22 ¹⁰Department of Organismic and Evolutionary Biology, Harvard University, Cambridge,
23 MA, USA

24 ¹¹USDA ARS Southwest Watershed Research Center, Tucson, AZ, USA

25 ¹²Global Modeling and Assimilation Office, NASA Goddard Space Flight Center,
26 Greenbelt, MD, USA

27 ¹³Jet Propulsion Laboratory, California Institute of Technology, Pasadena, CA, USA

28 ¹⁴Atmospheric Chemistry and Dynamics Laboratory, NASA Goddard Space Flight
29 Center, Greenbelt, MD, USA

30

31 **Abstract**

32 A frequently expressed viewpoint across the Earth science community is that global soil
33 moisture estimates from satellite L-band (1.4 GHz) measurements represent moisture
34 only in a shallow surface layer (0-5 cm) and consequently are of limited value for
35 studying global terrestrial ecosystems because plants use water from deeper rootzones.
36 Using this argumentation, many observation-based land surface studies avoid satellite-
37 observed soil moisture. Here, based on peer-reviewed literature across several fields,
38 we argue that such a viewpoint is overly limiting for two reasons. First, microwave soil
39 emission depth considerations and statistical considerations of vertically correlated soil
40 moisture information together indicate that L-band measurements carry information
41 about soil moisture extending below the commonly referenced 5 cm in many conditions.
42 However, spatial variations of effective depths of representation remain uncertain.
43 Second, in reviewing isotopic tracer field studies of plant water uptake, we find a
44 prevalence of vegetation that primarily draws moisture from these upper soil layers. This
45 is especially true for grasslands and croplands covering more than a third of global

46 vegetated surfaces. Even some deeper-rooted species (i.e., shrubs and trees)
47 preferentially or seasonally draw water from the upper soil layers. Therefore, L-band
48 satellite soil moisture estimates are more relevant to global vegetation water uptake
49 than commonly appreciated (i.e., relevant beyond only shallow soil processes like soil
50 evaporation). Our commentary encourages the application of satellite soil moisture
51 across a broader range of terrestrial hydrosphere and biosphere studies while urging
52 more rigorous estimates of its effective depth of representation.

53

54 **1. Introduction**

55 Global soil moisture retrievals from microwave satellites are now widely used across the
56 Earth science community to study various topics related to the global climate system
57 and its water, carbon, and energy cycles. While soil moisture in the unsaturated zone
58 stores only 0.005% of Earth's water by volume (Bras, 1990), its position at the interface
59 of the land and the atmosphere is of high value for understanding these global cycles
60 (Koster and Suarez, 2001; McColl et al., 2017). As such, satellite-based soil moisture
61 estimates are increasingly being used in studies of land-atmosphere interactions,
62 numerical weather prediction, plant function and stress, and land surface response to
63 climate change (Akbar et al., 2020; Dong et al., 2020; Feldman et al., 2022, 2018b;
64 Konings et al., 2017; Purdy et al., 2018; Santanello et al., 2019; Short Gianotti et al.,
65 2020; Taylor et al., 2012; Tuttle and Salvucci, 2016).

66

67 However, there is now a frequently expressed viewpoint that microwave satellite soil
68 moisture products are of limited use for studying vegetated landscapes because they
69 sense only a superficial fraction of the rootzone. Across global studies using satellite-
70 derived soil moisture, there is widespread, explicit mention of this limitation (Bassiouni
71 et al., 2020; Denissen et al., 2020; Ford et al., 2014; Peng et al., 2021, 2017; Qiu et al.,
72 2014; Sehgal et al., 2021). Some studies use this limitation as the basis for using
73 modeled rootzone soil moisture datasets instead of satellite observations for land
74 surface studies (Farahmand et al., 2021; Koster et al., 2019; Liu et al., 2020) or
75 alternatively estimating a rootzone soil moisture (Calvet and Noilhan, 2000; Ford et al.,
76 2014; Li et al., 2010; Scott et al., 2003). Others are less explicit, but may have similar
77 reasoning for avoiding use of satellite soil moisture and favoring precipitation-based
78 wetness indices or rootzone moisture products from model reanalysis (Li et al., 2021;
79 Mueller and Seneviratne, 2012; Zhou et al., 2021).

80

81 A major contributor to this viewpoint is the history of the microwave remote sensing
82 community generally offering a simplified view of a single, shallow observing depth of
83 satellite-based retrievals. Modeling and field studies have characterized microwave
84 emission profiles that are a function mainly of soil moisture (Shen et al., 2021; Tsang et
85 al., 1975; Ulaby and Long, 2014), but the emission profiles are commonly simplified to
86 single, conservative support scale values (see, for example, Wilheit, 1978). Reflecting
87 this, the Soil Moisture Active Passive (SMAP) and Soil Moisture and Ocean Salinity
88 (SMOS) L-band satellite missions are often described as producing estimates of soil
89 moisture within the top 5 cm of soil (Entekhabi et al., 2010; Kerr et al., 2010). Similarly,
90 the Advanced Microwave Scanning Radiometer (AMSR) satellite series and the
91 Advanced Scatterometer (ASCAT) (at higher C- and X-band frequencies) are thought to

92 observe only the top 1-2 cm of soil (Njoku et al., 2003). Other contributors to this
93 viewpoint include the prevalent use of the top-most in-situ sensors for assessing
94 satellite soil moisture products (Chan et al., 2016), and a simplified intuition that the
95 maximum rooting depth defines the relevant water uptake profile (Nippert and Holdo,
96 2015).

97
98 According to this viewpoint, if roots supply plants from soil layers down to maximum
99 rooting depths that are meters below the top 5 cm, then L-band satellite soil moisture
100 estimates have little value for the global study of terrestrial water, carbon, and energy
101 fluxes, given that these fluxes can rely heavily on plant use of soil moisture (Jasechko et
102 al., 2013; Katul et al., 2012). If satellite soil moisture retrievals were to hold more
103 information about the rootzone, they could be considered more desirable than
104 reanalysis products for some observation-based land-atmosphere and ecological
105 applications; they are observations independent of model-prescribed linkages with other
106 land surface variables and provide direct information about plant water use and
107 evapotranspiration (Dong and Crow, 2019).

108
109 In fact, current evidence from soil moisture vertical coupling studies as well as
110 microwave emission modeling and field experiments suggests that L-band satellite
111 retrievals often represent soil moisture below the shallow (0-5 cm) surface soil layer.
112 Under drier soil conditions, microwave emission models and field measurements show
113 that microwave emission originates from layers below a depth of 5 cm (Liu et al., 2016;
114 Lv et al., 2018; Moghaddam et al., 2000; Ulaby and Long, 2014). Under wetter soil
115 conditions, studies show surface and rootzone moisture dynamics are often
116 hydraulically connected and correlated despite soil evaporation acting to decouple these
117 layers (Akbar et al., 2018; Ford et al., 2014; Qiu et al., 2014). This is because rootzone
118 moisture is driven by surface forcing and has strong spatiotemporal memory resulting in
119 similar soil moisture dynamics in the upper surface and deeper soil layers (though these
120 conditions are reduced in dry climates with strong seasonal drying and consequent
121 decoupling of upper and deeper soil layers) (Albergel et al., 2008; Crow et al., 2017;
122 McColl et al., 2017). As a result, the effective vertical depth of representation, or support
123 scale, of L-band satellite soil moisture retrievals have been shown to be deeper than 5
124 cm for wetter, coupled soil conditions (Akbar et al., 2018; Short Gianotti et al., 2019).

125
126 Furthermore, part of the argument to reject use of satellite soil moisture is an emphasis
127 on the fact that maximum rooting depths can extend plant water uptake meters into the
128 soil (Nepstad et al., 1994). However, this notion neglects the fact that active water
129 uptake is rarely uniform across the rooting profile (Nippert and Holdo, 2015).

130 Specifically, global observations and optimally modeled rooting profiles indicate that a
131 large proportion of plants preferentially draw water from the upper soil layers to take
132 advantage of these layers' pulse water and nutrient availability (Collins and Bras, 2007;
133 Jackson et al., 1996; Nippert and Holdo, 2015). As such, not only soil evaporation, but
134 also root water uptake can conceivably influence these upper soil layer moisture
135 dynamics. Even for deeper-rooted vegetation, high sensitivity to upper-layer soil
136 moisture is also found based on findings of decreasing rooting biomass and root
137 hydraulic conductance with depth (Nippert et al., 2012; Werner et al., 2021). Therefore,

138 to learn about nominal plant water use and evapotranspiration, rootzone soil moisture
139 products may not always need to integrate moisture dynamics down to the maximum
140 rooting depth.

141
142 Here, we ask: do L-band microwave remote sensing products only represent soil
143 moisture in the top 0-5 cm? Can L-band satellite soil moisture retrievals be useful for
144 studying plant water use and, if so, under what conditions? In this commentary, we
145 provide a novel synthesis of results from microwave remote sensing, soil hydrology, and
146 plant water isotopic tracer studies to illustrate that satellite soil moisture observations
147 are more useful than commonly believed for studying global vegetated surfaces.
148

149 **2. Satellite Soil Moisture's Effective Depth of Representation**

150 The true vertical support, or effective depth of representation, of remote sensing-based
151 soil moisture retrievals is dependent on both (1) the microwave emission properties of
152 the soil column and (2) the vertical autocorrelation of typical soil moisture profiles and
153 their dynamics (Njoku and Entekhabi, 1996; Short Gianotti et al., 2019). Both principles
154 typically result in the remote sensing signal being representative of a soil moisture
155 profile that decays with depth (e.g., exponential distribution). Therefore, reported single
156 depth values are length scales, or the depth at which the satellite signal holds a portion
157 (e.g., 63% for e-folding scales) of soil moisture information from the sensed profile with
158 some information coming from deeper layers. Furthermore, these principles trade off in
159 dominance from dry to wet conditions (Fig. 1). Ultimately, we argue here that evidence
160 for both principles results in effective L-band depths of representation deeper than 5 cm
161 across many conditions. Additionally, reported depths at a single value (e.g., 5 cm) are
162 not a limit, but rather length scales describing a profile of soil moisture representation
163 that continues below the reported value. A more quantitative discussion of satellite soil
164 moisture depths of representation is provided in Sections 2.1 and 2.2.
165

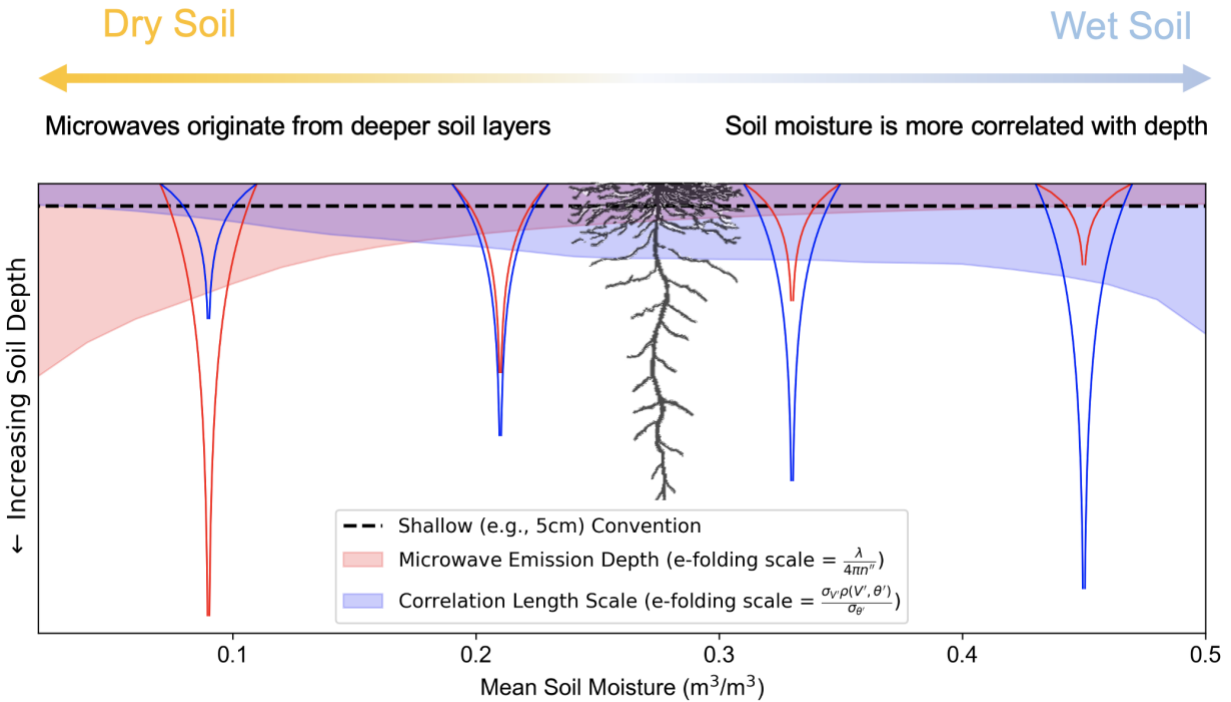
166 For drier soils, L-band satellites typically directly detect soil moisture in a deeper soil
167 column because microwave emission originates from deeper soil layers than for wetter
168 soils (Fig. 1). Specifically, modeling microwave emission from a soil layer that is
169 assumed to be a homogenous, dielectric medium with uniform moisture and
170 temperature profiles reveals that soil emission depth increases with aridity and vertically
171 decays approximately exponentially (Njoku and Entekhabi, 1996; Njoku and Kong,
172 1977). Therefore, despite drier periods resulting in less coupling between surface and
173 deeper layer soil moisture (Fig. 2), satellites should directly sample deeper into the soil
174 column for drier soils, where the emission likely originates partly below a depth of 5 cm
175 but can be hindered by fine soil texture and large soil scatterers. Microwave emission
176 depth e-folding scales in Fig. 1 are computed based on a soil emission model (Eq. A1,
177 which is from Njoku and Entekhabi, (1996)). See Section 2.1 for a more quantitative
178 discussion.
179

180 For wetter soils, despite shallower soil emission depths from an electromagnetic
181 perspective, surface soil moisture has a greater hydraulic connectivity with deeper soil
182 layers (Figs. 1 and 2). This is because soil moisture is a storage variable with strong
183 spatiotemporal memory (McColl et al., 2017). This memory results in daily soil moisture

184 variations at a 5 cm depth (the emission depth under wetter conditions) correlating with
185 deeper soil moisture variations. Such vertical autocorrelation information decays
186 approximately exponentially with depth (Fig. 1). E-folding vertical correlation length
187 scales reported in Fig. 1 are global remote sensing-based vertical length scales
188 estimated using Eq. A2 in Short Gianotti et al., (2019). See Section 2.2 for a more
189 quantitative discussion.

190
191 Combining these electromagnetic and statistical considerations suggests that, across
192 soil moisture conditions, L-band satellite soil moisture retrievals effectively carry
193 information about soil moisture dynamics deeper than 5 cm depending on the
194 subsurface conditions (Fig. 1). This deeper effective depth of representation results
195 from electromagnetic and statistical considerations of satellite-based soil moisture
196 trading off in their dominance of vertical soil representation from dry to wet conditions. In
197 principle, the combined support scale of the satellite-based soil moisture dynamics is at
198 least the deeper of the two considerations, and we urge future work to estimate holistic
199 effective depths of representation across the globe. Deeper layers well below 5 cm are
200 often still integrated but contribute progressively (i.e., exponentially) less to the effective
201 satellite soil moisture signal with depth (Figs. 1 and 2). By contrast, reanalysis rootzone
202 moisture products often assess the uniform, column-averaged soil moisture typically
203 between 0 and 100 cm and/or discretized portions of this range.

204
205 The modifier “effective” is used to describe the depth of representation here because
206 both direct and indirect sensing contributes to the estimated depth of representation. In
207 the case of drier soils, the microwave emission typically originates from layers deeper
208 than 5 cm (see Section 2.1), which would provide direct observation of the magnitude
209 and time variations of deeper layer soil moisture. However, in wetter conditions, only the
210 soil moisture magnitude and variations in the upper soil layers, likely shallower than 5
211 cm, are directly observed by L-band satellite sensors. Nevertheless, the typically high
212 hydraulic connectivity between shallow and deeper layers in these wetter conditions at
213 daily-to-weekly timescales allows indirect observation of the soil moisture magnitude
214 and variations in the deeper layers. As such, the vertical depth of representation is
215 indirect and more “effective” when using statistical arguments in wetter conditions.



216
 217 Figure 1. Effective depth of representation of microwave satellite soil moisture retrievals
 218 based on consideration of both microwave soil emission physics and vertical hydraulic
 219 connectivity of soil moisture. Satellite effective depths of representation of soil moisture
 220 likely extend deeper than 5 cm across many conditions at L-band. However, effective
 221 depths across space remain uncertain with current evidence discussed in Sections 2.1
 222 and 2.2. Note that single value depths refer to a profile of soil moisture representation;
 223 as examples shown in this diagram, effective depths of representation (red/blue
 224 shading) are e-folding scales determined from modeled microwave soil emission vertical
 225 distributions (red lines) and estimated soil moisture vertical correlation distributions
 226 (blue lines). Under drier conditions, microwave emission theoretically originates directly
 227 from deeper layers, while for wetter conditions, correlation length scale arguments only
 228 provide an effective representation of deeper soil layers. The diagram can scale
 229 depending on the frequency across low frequency microwaves. For equation details,
 230 see Appendix A. The displayed root profile image was adapted with permission from
 231 Nippert and Holdo, (2015). It has a commonly observed vertical structure of decreasing
 232 root biomass with depth. However, note that the length scale of this root density decay
 233 will vary globally.

234

235 **2.1 Depths of Representation Under Drier Conditions**

236 Microwave emission depth scales theoretically increase with drying soil (Burke et al.,
 237 1979; Ulaby and Long, 2014). However, estimates of emission depths under dry
 238 conditions as a function of soil texture remain uncertain with differences between model
 239 and experimental evidence. Ultimately, based on current evidence, we expect that the
 240 mean emission depth scales under dry soils are deeper than 5 cm under many
 241 conditions, and likely between the shallower experimentally determined values and
 242 deeper model-based values. Furthermore, given that microwave emission is based on

243 an emission profile (not a uniform profile with a cutoff), some emission will originate
244 from below the reported length scale values here (see profiles in Fig. 1).

245
246 Under dry soils, microwave emission models produce e-folding depth of representation
247 scales deeper than 5 cm, with estimates below 30 cm for the driest soils. This result
248 holds for a wide range of clay fraction values (Fig. 1 shows case of 20% clay fraction),
249 with soil texture only minimally impacting emission depth (Shen et al., 2021).
250 Furthermore, emission depth magnitudes from several different emission and dielectric
251 models tend to agree with that of Eq. A1 (Fluhrer et al., 2022; Lv et al., 2018; Njoku and
252 Entekhabi, 1996).

253
254 However, these model-based emission depth estimates are likely upper bounds. In
255 assuming homogenous media without an air-soil boundary, these emission models will
256 underestimate scattering effects (Zwieback et al., 2015). Specifically, scattering due to
257 the air-soil boundary and scattering from subsurface features at the scale of the
258 microwave wavelength within the medium will reduce the emission depth (Newton
259 1982). Formation of biocrusts, prevalent in global drylands (Phillips et al., 2022), and
260 near surface debris may also create scattering effects that will limit emission depths.
261 These models also assume uniform soil moisture and temperature with depth. However,
262 since soil commonly dries at the surface first, emission will only originate from the dry
263 upper layers and little from below the transition to wet layers (Shen et al., 2021).

264
265 Experimental studies suggest emission from deeper than 5 cm in dry conditions, but
266 results are variable without well-known dependencies. Some studies find emission
267 depths of 5-10 cm under drier soils, and potentially closer to 5 cm for soil with high clay
268 content (Lv et al., 2018; Owe and Van De Griend, 1998; Rao et al., 1988). Another finds
269 deeper soil moisture representation of near 100 cm (Moghaddam et al., 2000), though
270 this may be due to reduced scattering in more uniform sand (Mätzler, 1998). Others
271 suggest these emission depths may still be within the top 5 cm for dry soils similarly to
272 wetter soils (Escorihuela et al., 2010; Newton et al., 1982).

273
274 However, there are confounding factors in these experimental studies that likely cause
275 underestimations of dry soil sensing depths. Many field studies that suggest emission is
276 from shallower than 5 cm across conditions draw conclusions using a wide range of soil
277 moisture values (Escorihuela et al., 2010; Owe and Van De Griend, 1998; Shen et al.,
278 2021). These procedures will likely underestimate the dry soil emission depth by
279 including wet soils conditions. Additionally, some studies draw conclusions about
280 shallow emission depths without measuring soil moisture values below their depth
281 estimate and/or without explicitly showing that the soil moisture values below their depth
282 estimate contribute less to the signal (Escorihuela et al., 2010; Owe and Van De Griend,
283 1998). We argue that more targeted microwave experiments are needed to better
284 estimate the dry soil emission depths globally and their dependencies (see
285 recommendations in Section 5).

286
287 ***2.2 Effective Depths of Representation Under Wetter Conditions***

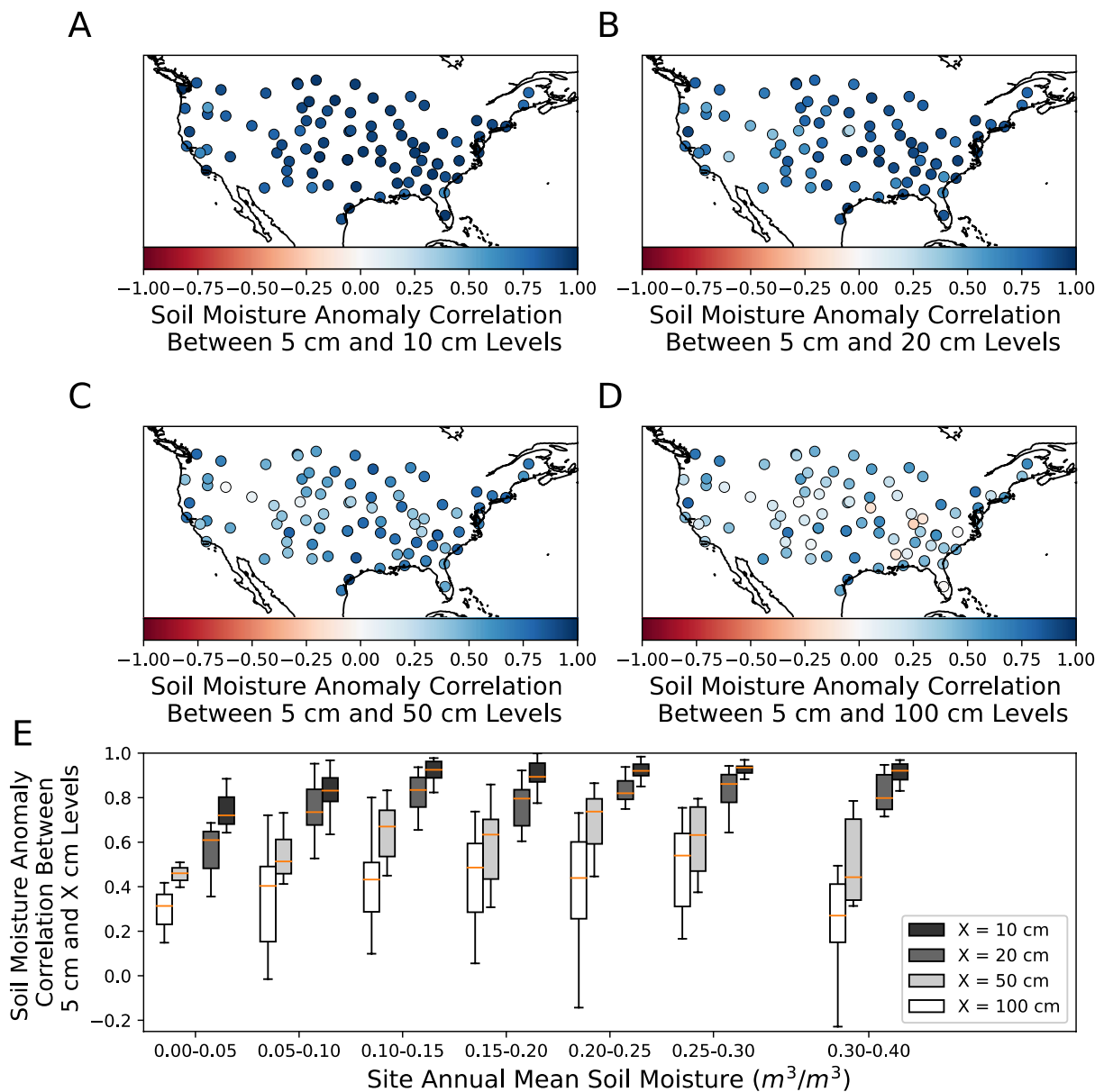
288 Under conditions ranging from moderately wet to very wet conditions, microwave field
289 experiments tend to find a 5 cm emission depth as measured by L-band radiometers,
290 suggesting that L-band satellites like SMAP and SMOS directly sense the first 5 cm of
291 soil with a weaker contribution of emission from deeper than 5 cm (Jackson et al., 1984;
292 Njoku and O'Neill, 1982; Wang, 1987). Some studies argue that L-band microwave
293 emission may only observe soil moisture in the first 2 cm of the soil (Escorihuela et al.,
294 2010; Schmugge, 1983; Wilheit, 1978). However, these findings of shallower emission
295 may be under scenarios of high air-soil interface roughness (Newton et al., 1982).
296 These results may also be uncertain due to interpretation of small correlation
297 differences between soil moisture and brightness temperature in different soil layers.
298

299 Nevertheless, soil moisture in the top few centimeters is typically well-correlated with
300 deeper soil layer moisture. Across wetter environments, in-situ soil moisture sensors
301 show high soil moisture anomaly correlations (>0.8) between 5 cm and depths of 10 cm
302 and 20 cm (Fig. 2). The correlation increases with higher mean soil moisture (Fig. 2E)
303 are consistent with the interpretation that the partially saturated soil hydraulic
304 conductivity increases with moisture content and allows redistribution of soil moisture
305 across the profile under matric and elevation head gradients. Consideration of lagged
306 correlations does not change the correlations appreciably, meaning much of the
307 subsurface coupling can be accounted for within daily dynamics. Using this concept, L-
308 band satellite soil moisture retrievals have been previously used to globally estimate
309 effective depths of representation, which tend to be deeper than 5 cm across wetter
310 conditions, but only rarely more than 30 cm (Akbar et al., 2018; Short Gianotti et al.,
311 2019). For deeper layers, these correlations can greatly decrease and even show
312 anticorrelations between anomalies in shallower and deeper soil layers (Fig. 2). More
313 detailed study is needed to quantify effective length scales and how they vary with soil
314 hydraulic conditions.
315

316 The vertically correlated nature of soil moisture under wetter conditions has emerged in
317 previous work. Surface soil moisture has been shown to have similar information
318 content as deeper layer soil moisture in explaining evapotranspiration fluxes and
319 moisture thresholds between evaporative regimes (Dong et al., 2022; Qiu et al., 2016).
320 Experimental microwave L-band field studies have found emission depths deeper than
321 5 cm under wetter conditions, but this may have been due to soil moisture being
322 correlated with depth (Macelloni et al., 2003; Pampaloni et al., 1990). Finally, L-band
323 satellite soil moisture was useful as a direct representation of rootzone conditions
324 deeper than 5 cm when modeling ecosystem carbon fluxes (Zhang et al., 2022).
325

326 C- and X-band (6.9 GHz and 10.7 GHz) depths of representation are shallower and
327 potentially have less utility for our arguments (Owe and Van De Griend, 1998; Wilheit,
328 1978). Namely, these wavelengths are about 5- and 8-times smaller than L-band,
329 respectively, which in principle result in 5- and 8-times shallower soil emission depths
330 (Eq. A1) across moisture and texture conditions. However, similar vertical soil moisture
331 correlation arguments can be applied to these higher C- and X-band frequencies under
332 wetter conditions. We encourage the analysis with Eq. A2 in the Short Gianotti et al.

333 (2019) study to be repeated with C- and X-band radiometer observations to estimate
 334 their correlation length scales.
 335



336
 337 Figure 2. Vertical correlations from in-situ USCRN measurements support that soil
 338 moisture in the upper 5 cm layers holds information about variations in rootzone soil
 339 layers under wetter soil moisture conditions. Soil moisture daily anomaly correlations
 340 between 5 cm sensor measurement depth and soil depths of (A) 10 cm, (B) 20 cm, (C)
 341 50 cm, and (D) 100 cm using U.S. Climate Reference Network (USCRN) soil moisture
 342 (Bell et al., 2013). (E) Spatial distributions of anomaly correlations from (A) to (D) panels
 343 with USCRN sites binned as a function of the sites' mean annual soil moisture.
 344

345 **3. Relevance of Satellite Soil Moisture Retrievals to Plant Water Uptake**

346 A frequently expressed argument when discouraging the use of satellite soil moisture is
347 that rootzones are (qualitatively) “deep,” which argues against using an upper rootzone
348 soil moisture dataset to study vegetated landscapes. Indeed, maximum rooting depths
349 often extend to 1-2-m and, at times, tens of meters below the surface depending on
350 climate, edaphic conditions, and topography (Fan et al., 2017; Nepstad et al., 1994;
351 Schenk and Jackson, 2002; Tumber-Dávila et al., 2022). Existence of deep roots
352 indicates adaptation to plant water stress, where access to deeper, less variable water
353 sources allows plants to continue transpiring to survive under seasonal or severe water
354 limitation (Jiang et al., 2020; Stocker et al., 2021; Tumber-Dávila and Malhotra, 2020).
355 However, in the context of nominal plant water uptake, such a perspective can result in
356 over-emphasis of the maximum rooting depth and neglect of the nature of typical rooting
357 profiles when discouraging the use of satellite soil moisture. Specifically, while there are
358 indeed many cases of deep root water use, global rooting profiles are often
359 concentrated in the upper soil layers and decrease in root density with depth (Jackson
360 et al., 1996). Some estimates indicate that most species (potentially as high as 90%),
361 and especially herbaceous plants, concentrate the majority of their roots in depths
362 shallower than 30 cm (Schenk and Jackson, 2002).

363
364 Due to root suberization and woody root development that prevents root water uptake,
365 the rooting distribution does not necessarily match the actual vertical profile of root
366 water uptake (Kramer and Boyer, 1995). Instead, isotopic tracers can be used to
367 estimate the true range of primary water uptake, commonly called the functional rooting
368 profile (Dawson and Pate, 1996; Ehleringer and Dawson, 1992). Within the limits
369 imposed by isotopic mixing model uncertainties (Case et al., 2020; Ogle et al., 2004),
370 isotopic tracer methods can determine water uptake profiles and/or ranges more
371 relevant to the water cycle than knowledge of the rooting profile alone.

372
373 Therefore, instead of rooting profile information, we have collated isotopic tracer studies
374 that determine the vertical range of roots contributing the most to xylem water within
375 plants (Fig. 3). Our main goal was to assess whether there are widespread cases of
376 plants using soil moisture that may be relevant to L-band satellite representation of
377 upper layer soil moisture. Values displayed in Fig. 3 reflect the primary zones of water
378 uptake over most of the year indicated by each reviewed study. In our web search of
379 peer-reviewed literature, our keywords included “stable”, “isotope,” “tracer,” “plant,”
380 “root,” “water uptake,” and “soil.” We only sampled studies that (a) explicitly stated or
381 displayed the primary depths of water uptake (avoiding subjective judgment of results),
382 (b) assessed naturally occurring plants under nominal conditions (avoiding experimental
383 manipulation, extreme stress, and laboratory experiments), and (c) evaluated plant
384 species with an unobstructed rootzone (avoiding riparian, coastal, and shallow bedrock
385 environments). Our search resulted in 45 references that met our criteria (Fig. 3 and
386 Table S1).

387
388 We find that grass and crop species (primarily herbaceous) across global climates
389 typically extract water from the upper soil layers (shallower than 25 or 30 cm) over most
390 of the year, with preferential uptake of water nearer to the surface (Figs. 3A and 3B).
391 70% of studied grass species typically use water in the upper 30 cm of soil. 65% of

392 grass studies find increased proportional uptake in the top-most soil layers, with many
393 explicitly reporting use of water at 0-5 cm depths (Fig. 3A). While 43% of studied crop
394 species use water mainly shallower than 25 cm, all sampled crop species preferentially
395 draw water from the upper soil layers with decreasing water use with depth (Fig. 3B). All
396 crop studies that found water use extending deeper than 50 cm also found
397 proportionally higher water use in the upper soil layers. 88% of these same studies also
398 found the primary plant water uptake zone transitioned at least temporarily to the upper
399 soil layers (see diamond symbols in Fig. 3B).

400
401 Shrub and tree species show a larger vertical range of water uptake, with water uptake
402 commonly extending to well below 50 cm (Figs. 3C and 3D) often related to root-niche
403 separation under competition with grasses (Case et al., 2020). However, even in these
404 deeper water uptake cases, 89% of shrub and 67% of tree isotopic studies found either
405 proportionally higher water uptake from the upper soil layers or the primary water use
406 zone transitioned temporarily to the upper soil layers. Absence of triangle and diamond
407 symbols indicate that the study did not mention either phenomenon, not that the
408 phenomenon does not exist. Therefore, these percentages that indicate preferential or
409 temporary uptake of upper soil layer moisture are lower bounds.

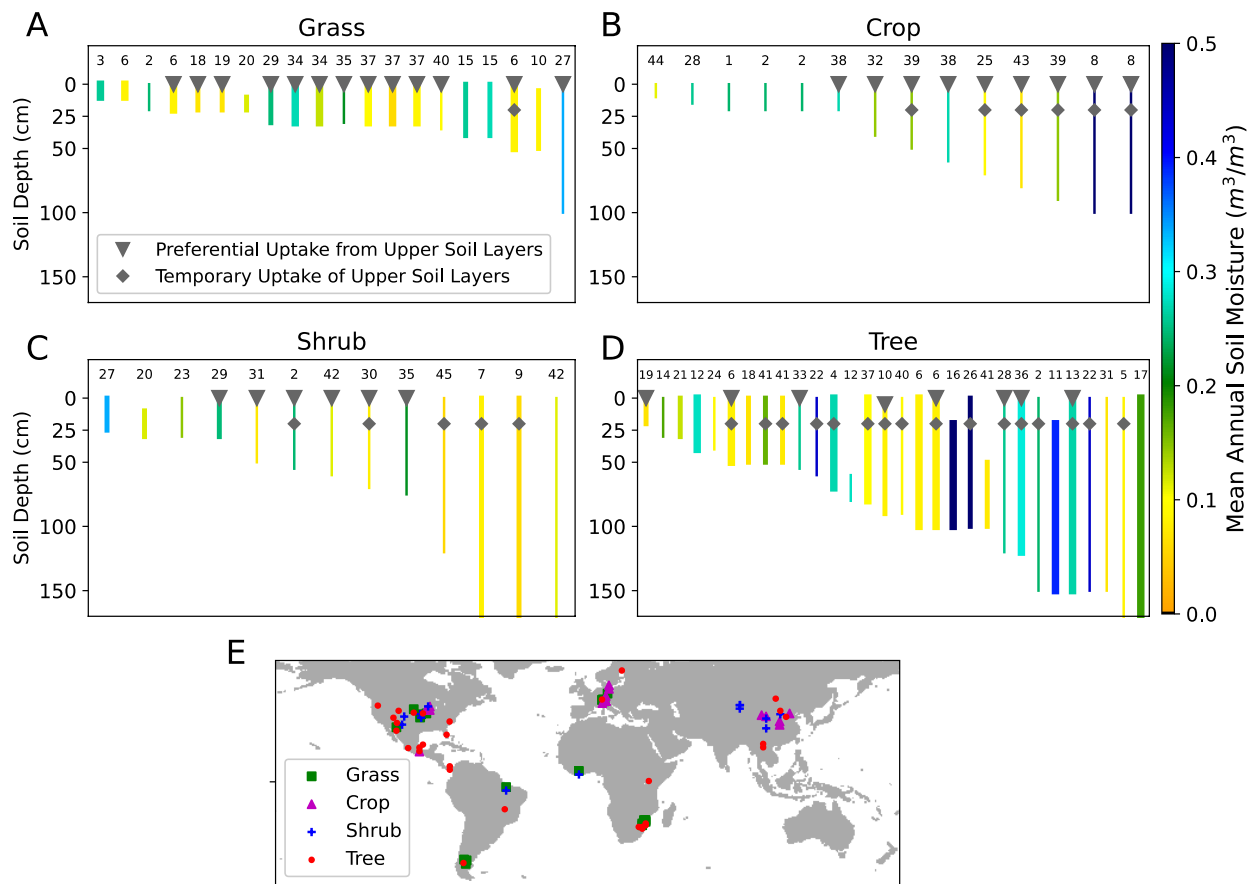
410
411 We acknowledge potential biases in our search. For example, a greater proportion of
412 studies in the midlatitudes arises due to abundant field research facilities in Asia,
413 Europe, and North America as well as due to a lack of field measurements in the tropics
414 (Schimel et al., 2015). More studies also take place in semi-arid and sub-humid
415 environments because of their higher proportion of global land cover. While our search
416 yielded few tropical forest studies, we expect these regions may have deeper functional
417 rooting profiles similarly to those found in Fig. 3D (Ichii et al., 2007). However, we argue
418 that this search provided a representative distribution of species across grass, crop,
419 shrub, and tree categories and across global moisture availability gradients.

420
421 Though roots and consequent root water uptake profiles can extend below 30 cm, likely
422 beyond the profiles of L-band satellite soil moisture representation (especially for shrubs
423 and trees), our analysis shows that shallow root water uptake is widespread (Figure 3).
424 Furthermore, even in the presence of deep roots, this analysis shows that shallow
425 preferential soil water uptake and deeper roots can exist concurrently – the existence of
426 a deep maximum rooting depth does not always imply low plant utilization of shallow
427 soil moisture. This claim is supported by previous estimates that root water use from
428 deeper layers may be smaller, or less than 10% of annual plant water uptake
429 (McCormick et al., 2021; Miguez-Macho and Fan, 2021). This lower contribution of
430 water uptake from the deeper layers may be, in part, because there are hydraulic
431 limitations in transporting water over long vertical distances from deeper roots, with high
432 radial and axial resistances in roots that can increase with depth (Jones, 2014;
433 Landsberg and Fowkes, 1978; Nippert et al., 2012). As such, deeper roots may be more
434 important for survival under seasonal or severe water limitation rather than nominal
435 uptake (Stocker et al., 2021; Wang-Erlandsson et al., 2016). Use of deeper roots is
436 limited in many water-limited ecosystems (Nippert and Holdo, 2015), where rainfall
437 infiltration is often shallow (<30 cm) and plants must rely on this more frequently wetted

438 shallow zone for survival (Scott and Biederman, 2019). Additionally, essential limiting
 439 nutrients are typically highly concentrated in the upper soil layers due to decaying
 440 organic matter, which may prevent sole plant reliance on deeper moisture sources
 441 (Jobbágy and Jackson, 2001). This motivates strategies like hydraulic redistribution
 442 where plants actively move water via the roots to upper soil layers for easier uptake of
 443 nutrients under dry conditions (Cardon et al., 2013). As such, knowledge of maximum
 444 rooting depths should be used with caution when evaluating nominal plant water uptake
 445 throughout the year in the context of global soil moisture estimates (Nippert and Holdo,
 446 2015).

447
 448 This evidence together with Section 2 ultimately indicates that plant water use of upper
 449 soil layers is likely prevalent within a satellite pixel in some biomes, especially those
 450 with herbaceous vegetation, and highlights the utility of L-band satellite soil moisture for
 451 studying water control of many vegetated surfaces. We stress that we are not making
 452 wider claims about global dominance of shallow plant uptake strategies, but rather that
 453 deep root water use may be overemphasized when discussing limitations of using
 454 satellite soil moisture to study the terrestrial biosphere.

455



456
 457 Figure 3. Primary root water uptake profiles (or functional rooting profile) based on field
 458 stable isotope tracer studies for species binned in (A) grass, (B) crop, (C) shrub, and (D)
 459 tree categories based on Table S1 and dataset in Feldman et al., (2023). The triangle

460 symbol means the study found preferential water uptake nearer to the surface and
461 decreasing uptake with depth. The diamond symbol means that while the study found
462 uptake to 50 cm soil depths or below, root water uptake switched primarily to the upper
463 soil layers (<~30cm) temporarily during the year. Placement of the diamond symbol at
464 20 cm is arbitrary. Thickness of the line indicates number of species studied in the given
465 reference. The number above the plotlines is the reference index (see Table S1). The
466 line colors refer to the mean annual SMAP soil moisture shown in the colorbar for each
467 field site using the nearest 36 km pixel. (E) Locations of the isotopic field
468 measurements.

469

470 **4. Effective Depth of Representation Limitations**

471 Several soil and vegetation processes can limit L-band retrievals effectively capturing
472 soil moisture dynamics from deeper than 5 cm. We discuss several limitations here and
473 comment on whether our arguments are confounded by or robust to these processes.

474

475 Regarding microwave soil emission depth arguments in dry conditions, large subsurface
476 scatterers, like woody roots and rock inclusions that are larger than the wavelength of L-
477 band microwaves (~20 cm) can reduce the depth of soil microwave emission (Roth and
478 Elachi, 1975; Xiong et al., 2017). This is especially the case if belowground rooting
479 density and rock inclusions are present across the satellite footprint. Deeper soil
480 emission may occur in many drier regions (Section 2.1), which climatically tend to have
481 lower woody vegetation density and thus may be less consistently influenced by larger
482 roots (Good and Caylor, 2011). However, the existence of large abiotic soil scatterers
483 across a satellite footprint can reduce the depth of microwave soil emission, in which
484 case modeled dry soil emission depth values are an overestimate. The global
485 distribution of soil scatterer density is uncertain and it is ultimately unclear how soil
486 texture heterogeneity at small spatial scales translates to uncertainties for our larger
487 scale arguments (Baroni et al., 2017; Or, 2020).

488

489 Regarding vertical correlation arguments in wet conditions, soil conditions that promote
490 heterogeneous vertical moisture movement rates in the subsurface can decouple
491 surface and deeper soil layers. This includes bare soil evaporation (i.e., the formation of
492 an evaporation front). A soil evaporation front forms with differential bare soil drying of
493 upper soil layers, which can act to decouple the near surface soil moisture dynamics
494 from the rootzone especially over long seasonal drydowns in seasonally dry
495 environments (Scott and Biederman, 2019). Nevertheless, macropores (Vereecken et
496 al., 2022) and processes like hydraulic redistribution of moisture from wet to dry soils by
497 roots of some plant species (Katul and Siqueira, 2010; Nadezhdina et al., 2010) could
498 act to further couple the surface and deeper soil layers. Macropores are large soil pore
499 spaces that make up less than 1% of soil volume, but can dominate gravity drainage
500 rates in the soil under wet conditions (Fatichi et al., 2020; Hirmas et al., 2018; Kramer
501 and Boyer, 1995). Ultimately, our arguments that shallow soil moisture under wet
502 conditions captures moisture dynamics of deeper than 5 cm due to vertical correlation
503 are based on satellite and in-situ observations, and thus they already integrate these
504 soil and vegetation processes and their limitations (Figs. 1 and 2).

505

506 Soil evaporation influences soil moisture at depths between 0 and 80 cm depending on
507 soil texture (Aminzadeh and Or, 2014; Lehmann et al., 2008; Or and Lehmann, 2019).
508 As such, near-surface soil moisture dynamics will have a signature of soil evaporation
509 physics (Haghighi et al., 2013; Salvucci, 1997). However, the existence of soil
510 evaporation in the upper soil layers does not preclude root water uptake from being
511 sensitive to upper rootzone soil moisture, including 0-5 cm. Our analysis indicates that
512 many plant species prefer moisture in upper soil layers (Fig. 3), with many isotopic
513 studies finding dominant uptake from 0-5 cm (Asbjornsen et al., 2008; Case et al., 2020;
514 Kulmatiski et al., 2010; Kulmatiski and Beard, 2013; Le Roux et al., 1995; Ogle et al.,
515 2004; Prechsl et al., 2015). As such, soil moisture in these upper layers is indeed
516 influenced by root water uptake along with bare soil evaporation in many cases. It is
517 also not likely that either bare soil or root water uptake entirely dominate globally given
518 estimates of transpiration and evaporation partitioning (Fatichi and Pappas, 2017; Good
519 et al., 2015; Jasechko et al., 2013). Remotely sensed soil moisture dynamics are thus a
520 function of both root water uptake and bare soil evaporation processes, but future work
521 should determine how much soil moisture dynamics in these layers is explained by plant
522 water uptake.

523
524 Aboveground vegetation biomass, from a passive microwave emission perspective,
525 does not necessarily impact the soil microwave emission profile and depth. Dense,
526 wooded vegetation canopies de-polarize the strongly horizontally and vertically
527 polarized soil microwave emission signal, where multiple-scattering of microwave
528 emission through the canopy reduces sensitivity to soil reflectivity and thus to soil
529 moisture (Feldman et al., 2018a; Kurum et al., 2011). Therefore, dense vegetation
530 results in a higher soil moisture retrieval error variance (Feldman et al., 2021; Zwieback
531 et al., 2019), but does not directly change the physics of electromagnetic attenuation in
532 the soil, and thus does not change the depth of microwave emission. Nevertheless, our
533 deeper direct microwave emission depth arguments pertain to dry soil conditions
534 (Section 2.1), where vegetation density tends to be lower and would thus be less
535 influenced by vegetation presence.

536

537 **5. Conclusions and Recommendations**

538 Our findings convey that satellite L-band retrievals effectively capture global soil
539 moisture dynamics deeper than 5 cm in many conditions (Section 2) and are more
540 relevant for evaluating plant function than commonly appreciated (Section 3). We find
541 that L-band satellite soil moisture retrievals will likely have their highest utility for
542 studying most grasslands and croplands, which cover more than a third of global
543 vegetated surfaces. This land cover proportion is higher when including non-vegetated
544 surfaces, given that these L-band measurements also have utility for evaluating bare
545 surfaces where soil evaporation dominates. Grass and crop water use also decreases
546 with depth, much like the decreasing L-band satellite soil moisture representation with
547 depth (Fig. 1). Therefore, reanalysis soil moisture datasets that integrate rootzone
548 dynamics between 0-100 cm and deeper may in fact be less useful than L-band soil
549 moisture for representing plant-relevant soil moisture dynamics in grass and croplands
550 (Fig. 3). This is because soil moisture products representing the 0-100 cm layer will
551 integrate subdued moisture dynamics in deeper layers not relevant to the functional

552 rooting profile concentrated in the upper soil layers. Additionally, even woody plant
553 species that exhibit deeper root water uptake (shrubs and trees; see Fig. 3) frequently
554 draw water nearer to the surface preferentially or temporarily within a given season. L-
555 band soil moisture observations are still useful for these scenarios at least during
556 certain times of the year.

557
558 We stress that deeper-layer (0-100 cm and beyond) soil moisture products based on the
559 assimilation of L-band observations (i.e., SMAP L4 rootzone soil moisture; Reichle et
560 al., 2019) are likely more optimal for the study of soil moisture memory in the context of
561 land-atmosphere interactions, the study of deeper-rooted vegetation function under
562 water-stress conditions, the study of infiltration and drainage fluxes, and the initialization
563 of dynamical seasonal forecasts. Our findings here also indicate that reanalysis
564 rootzone soil moisture products are needed for the study of many forested and mixed
565 (i.e., savanna) landscapes that have deeper plant water uptake and often higher errors
566 in remote sensing soil moisture retrievals.

567
568 Additionally, we argue that there is no single global soil moisture product that will
569 integrate the soil moisture layers relevant to plant water uptake and thus terrestrial
570 water, carbon, and energy exchanges. Instead, the optimal soil moisture product
571 changes in time and space. For studies of water, carbon, and energy exchanges at
572 landscape scales, we encourage first understanding the typical root water uptake
573 patterns for plant species in the study region and then carefully selecting a soil moisture
574 dataset. Potentially, multiple products and their synergistic use are needed depending
575 on the complexity of root water uptake scenarios.

576
577 For example, for landscapes with primarily herbaceous vegetation including many
578 croplands, grasslands, and savannas with sparse tree cover, the L-band soil moisture
579 products are more optimal for integrating the relevant rootzone moisture information
580 because they are typically sensitive to the shallow rootzone layers and often
581 progressively decrease in sensitivity to deeper soil moisture, much like these
582 ecosystem's functional rooting profiles. These observations will additionally be optimal
583 for the study of mostly bare surface supplied mainly by soil evaporation. Alternatively, in
584 scenarios where prevalent deeper-rooted shrubs and trees are mixed with a shallow-
585 rooted understory, datasets representing a uniform distribution of integrated soil
586 moisture across the top 1-2 meters of soil (i.e., model reanalysis rootzone soil moisture
587 products) would be optimal (Reichle et al., 2019). P-band (0.4 GHz) soil moisture
588 remote sensing applications may be useful for these scenarios as well - with potentially
589 twice as deep of effective depths of representation than at L-band and less sensitivity to
590 the overlying vegetation (Chapin et al., 2012; Konings et al., 2014; Shen et al., 2021).
591 These datasets may be similarly useful for plant water stress scenarios if the given
592 vegetation shifts its water use to deeper layers. Finally, in scenarios where root water
593 uptake extends well below one meter for consistent or transient use of deep moisture or
594 groundwater (McCormick et al., 2021; Miguez-Macho and Fan, 2021), care must be
595 taken in determining when this uptake occurs. Such scenarios may occur in tropical
596 rainforests where L-band satellite soil moisture retrievals are suboptimal due to
597 vegetation multiple-scattering of microwaves (Feldman et al., 2018a; Kurum et al.,

598 2011). Satellite-based terrestrial water storage variations (i.e., GRACE and GRACE-FO)
599 may be useful to study these cases and can be used in tandem with reanalysis rootzone
600 products (Rodell and Famiglietti, 2001).

601
602 Our commentary ultimately encourages broader use of L-band satellite soil moisture for
603 the study of soil moisture's impact on the terrestrial net carbon balance, water
604 movement in the soil-plant-atmosphere continuum, land-atmosphere coupling, and crop
605 yield forecasting. This is the case for grasslands and some croplands but may only
606 extend to woody biomes in some contexts. Based on the evidence presented here, we
607 argue that L-band satellite soil moisture is more useful than suggested by the frequently
608 assumed skin depth support scale. Furthermore, satellite soil moisture retrievals can
609 often serve as a more direct observation of relevant upper rootzone soil moisture than
610 less direct precipitation wetness indices or modeled rootzone products which may
611 include process assumptions that confound interpretations of emergent terrestrial
612 behavior.

613
614 With the availability of X-, C-, and L-band soil moisture observations, we urge more
615 study into quantifying effective depths of representation at each frequency and how they
616 change with soil structure and moisture across the globe. These estimates should
617 consider both microwave soil emission depths and statistical vertical correlation
618 arguments because previous studies evaluate these considerations in isolation (Lv et
619 al., 2018; Njoku and Kong, 1977; Short Gianotti et al., 2019). Correlative evidence
620 between brightness temperature and soil moisture across many depths can
621 simultaneously capture both the direct emission depths within the radiometric brightness
622 temperature measurements and the effective, vertical connections within the soil
623 moisture measurements. Furthermore, to draw more conclusive evidence about L-band
624 sensing depths under drier soils, we recommend that (1) microwave emission models
625 used to estimate sensing depths should be adapted to account for air-soil boundary and
626 within-layer scattering due to soil heterogeneity. (2) Field experiments should explicitly
627 test dry soil conditions without using methods that include wet soil conditions. Drydown
628 experiments as shown in a previous experiment may be useful in this endeavor (Newton
629 et al., 1982). (3) Field experiments should also establish that soil moisture from deeper
630 layers contributes much less to the signal in order to define a depth of representation.

631
632 Finally, the potential value of satellite-based soil moisture deeper than a 5 cm skin
633 depth highlights the need to maintain continuity of L-band satellite remote sensing
634 missions. Additionally, we have discussed several factors that limit the effective L-band
635 depth of soil representation, which motivate the need to directly observe deeper soil
636 moisture layers with upcoming satellite missions. We namely advocate for P-band
637 satellite soil moisture missions that can directly detect several times the effective L-band
638 depth of representation. Planned P-band missions include the European Space
639 Agency's BIOMASS mission and NASA's Signals of Opportunity P-band Investigation
640 (SNOOPI) (Garrison et al., 2019; Quegan et al., 2019).

641
642 **Appendix A**

643 The e-folding length scale of microwave emission used to estimate surface soil moisture
644 can be modeled by:

$$645 \quad L_{Emission} = \frac{\lambda}{4\pi n''} \quad (\text{Eq. A1})$$

646 where λ is the emission wavelength (Njoku and Entekhabi, 1996). n'' is the imaginary
647 part of the refractive index, which is the square root of the dielectric constant. The
648 dielectric constant is a function largely of soil moisture and soil texture (i.e., clay
649 fraction), though soil texture has smaller influences (Shen et al., 2021). Incidence
650 angles are not explicitly considered in these models, the consequences of which are not
651 well known (Shen et al., 2021). $L_{Emission}$ is the e-folding scale that represents the
652 emission depth of microwaves. Measurements of these microwaves are used to
653 estimate satellite soil moisture. Nearly identical emission length scales are found when
654 using other common emission and dielectric models (Fluhrer et al., 2022; Lv et al.,
655 2018).

656
657 The e-folding vertical correlation length scale of soil moisture dynamics can be
658 computed by:

$$659 \quad L_{Correlation} = \frac{\sigma_{V'} \rho(V', \theta_s')}{\sigma_{\theta_s'}} \quad (\text{Eq. A2})$$

660 where V is the total volume soil moisture in the column, θ_s is the surface soil moisture, ρ
661 is correlation, and σ is standard deviation (Short Gianotti et al., 2019). Prime
662 superscripts indicate the time derivative. $L_{Correlation}$ is a correlation length scale, or the e-
663 folding scale, that captures the decay of surface soil moisture's correlation with the total
664 column soil moisture. $L_{Correlation}$ is thus the effective depth to which the surface soil
665 moisture (here, being measured at least at a 5 cm depth) holds information about the
666 total soil column moisture. Similar theoretical arguments allow interpretation of $L_{Correlation}$
667 to be a support scale of the soil moisture magnitude and time dynamics (Akbar et al.,
668 2018).

669
670 While Eq. A2 is an exact solution, total column volumetric moisture is not widely
671 available to estimate $L_{Correlation}$ globally. Thus, Short Gianotti et al. (2019) estimate
672 $L_{Correlation}$ using information about the variance of surface hydrologic fluxes (rainfall
673 minus surface hydrologic losses) as well as surface soil moisture variance and
674 autocorrelation (their equation 28). GPM rainfall retrievals (Huffman, 2015) and SMAP
675 soil moisture retrievals are used together to globally estimate $L_{Correlation}$, which are used
676 in Fig. 1.

677

678 **Acknowledgements**

679 Andrew F. Feldman's research was supported by an appointment to the NASA
680 Postdoctoral Program at the NASA Goddard Space Flight Center, administered by Oak
681 Ridge Associated Universities under contract with NASA. The authors with MIT
682 affiliation, Rolf H. Reichle, and Wade T. Crow were supported by the NASA SMAP
683 mission. The authors thank the associate editor and three anonymous reviewers for
684 constructive comments that improved our manuscript. The USDA is an equal
685 opportunity employer.

686

687 **Author Contributions**

688 A.F.F. and D.E. conceived of and led the study. A.F.F. performed the analysis and
689 drafted the manuscript. D.J.S.G., J.D., R.A., W.T.C, A.G.K., and D.E. provided guidance
690 and edits on the presentation of satellite depth of representation estimates. J.B.N.,
691 S.J.T.D, N.M.H., F.E.R., and R.L.S. provided guidance and edits on presentation of
692 isotopic tracer studies and rooting depth information. K.A.M., R.H.R., A.C., J.J., and
693 B.P. provided guidance on all components and, in particular, in framing the perspective
694 in the context of their respective fields. All authors contributed substantial textual edits.
695

696 **Open Research**

697 **Data Availability Statement**

698 All data used in this study are freely and publicly available. In-situ USCRN soil moisture
699 observations were obtained from NOAA (<https://www.ncei.noaa.gov/access/crn/>). All
700 isotopic uptake profiles were determined from previous work with the data table stored
701 in <https://doi.org/10.5281/zenodo.7527459> and shown in Table S1. $L_{\text{Correlation}}$ length
702 scale estimates were obtained from Short Gianotti et al. (2019) and are included in
703 <https://doi.org/10.5281/zenodo.7527459>.
704

705 **Software Availability Statement**

706 No software was used or generated in this commentary.
707

708 **References**

- 709 Akbar, R., Short Gianotti, D., McColl, K.A., Haghghi, E., Salvucci, G.D., Entekhabi, D.,
710 2018. Hydrological Storage Length Scales Represented by Remote Sensing
711 Estimates of Soil Moisture and Precipitation. *Water Resour. Res.* 1476–1492.
712 <https://doi.org/10.1002/2017WR021508>
- 713 Akbar, R., Short Gianotti, D.J., Salvucci, G.D., Entekhabi, D., 2020. Partitioning of
714 Historical Precipitation Into Evaporation and Runoff Based on Hydrologic Dynamics
715 Identified With Recent SMAP Satellite Measurements. *Water Resour. Res.* 56, 1–
716 21. <https://doi.org/10.1029/2020WR027307>
- 717 Albergel, C., Rüdiger, C., Pellarin, T., Calvet, J.C., Fritz, N., Froissard, F., Suquia, D.,
718 Petitpa, A., Pignatelli, B., Martin, E., 2008. From near-surface to root-zone soil
719 moisture using an exponential filter: An assessment of the method based on in-situ
720 observations and model simulations. *Hydrol. Earth Syst. Sci.* 12, 1323–1337.
721 <https://doi.org/10.5194/hess-12-1323-2008>
- 722 Aminzadeh, M., Or, D., 2014. Energy partitioning dynamics of drying terrestrial surfaces.
723 *J. Hydrol.* 519, 1257–1270. <https://doi.org/10.1016/j.jhydrol.2014.08.037>
- 724 Asbjornsen, H., Shepherd, G., Helmers, M., Mora, G., 2008. Seasonal patterns in depth
725 of water uptake under contrasting annual and perennial systems in the Corn Belt
726 Region of the Midwestern U.S. *Plant Soil* 308, 69–92.
727 <https://doi.org/10.1007/s11104-008-9607-3>
- 728 Baroni, G., Zink, M., Kumar, R., Samaniego, L., Attinger, S., 2017. Effects of uncertainty
729 in soil properties on simulated hydrological states and fluxes at different spatio-
730 temporal scales. *Hydrol. Earth Syst. Sci.* 21, 2301–2320.
731 <https://doi.org/10.5194/hess-21-2301-2017>
- 732 Bassiouni, M., Good, S.P., Still, C.J., Higgins, C.W., 2020. Plant Water Uptake
733 Thresholds Inferred From Satellite Soil Moisture. *Geophys. Res. Lett.* 47, 1–12.

734 <https://doi.org/10.1029/2020GL087077>
735 Bell, J.E., Palecki, M.A., Baker, C.B., Collins, W.G., Lawrimore, J.H., Leeper, R.D., Hall,
736 M.E., Kochendorfer, J., Meyers, T.P., Wilson, T., Diamond, H.J., 2013. U.S. climate
737 reference network soil moisture and temperature observations. *J. Hydrometeorol.*
738 14, 977–988. <https://doi.org/10.1175/JHM-D-12-0146.1>
739 Bras, R.L., 1990. *Hydrology: An Introduction to Hydrologic Science*. Addison-Wesley
740 Publishing Co., Inc.
741 Burke, W.J., Schmugge, T., Paris, J.F., 1979. Comparison of 2.8- and 21-cm Microwave
742 Radiometer Observations Over Soils With Emission Model Calculations. *J.*
743 *Geophys. Res.* 84, 287–294.
744 Calvet, J.C., Noilhan, J., 2000. From near-surface to root-zone soil moisture using year-
745 round data. *J. Hydrometeorol.* 1, 393–411. [https://doi.org/10.1175/1525-](https://doi.org/10.1175/1525-7541(2000)001<0393:FNSTRZ>2.0.CO;2)
746 [7541\(2000\)001<0393:FNSTRZ>2.0.CO;2](https://doi.org/10.1175/1525-7541(2000)001<0393:FNSTRZ>2.0.CO;2)
747 Cardon, Z.G., Stark, J.M., Herron, P.M., Rasmussen, J.A., 2013. Sagebrush carrying
748 out hydraulic lift enhances surface soil nitrogen cycling and nitrogen uptake into
749 inflorescences. *Proc. Natl. Acad. Sci. U. S. A.* 110, 18988–18993.
750 <https://doi.org/10.1073/pnas.1311314110>
751 Case, M.F., Nippert, J.B., Holdo, R.M., Staver, A.C., 2020. Root-niche separation
752 between savanna trees and grasses is greater on sandier soils. *J. Ecol.* 108, 2298–
753 2308. <https://doi.org/10.1111/1365-2745.13475>
754 Chan, S.K., Bindlish, R., O'Neill, P.E., Njoku, E., Jackson, T., Colliander, A., Chen, F.,
755 Burgin, M., Dunbar, S., Piepmeier, J., Yueh, S., Entekhabi, D., Cosh, M.H.,
756 Caldwell, T., Walker, J., Wu, X., Berg, A., Rowlandson, T., Pacheco, A., McNairn,
757 H., Thibeault, M., Martinez-Fernandez, J., Gonzalez-Zamora, A., Seyfried, M.,
758 Bosch, D., Starks, P., Goodrich, D., Prueger, J., Palecki, M., Small, E.E., Zreda, M.,
759 Calvet, J.C., Crow, W.T., Kerr, Y., 2016. Assessment of the SMAP Passive Soil
760 Moisture Product. *IEEE Trans. Geosci. Remote Sens.* 54, 4994–5007.
761 <https://doi.org/10.1109/TGRS.2016.2561938>
762 Chapin, E., Chau, A., Chen, J., Heavey, B., Hensley, S., Lou, Y., Machuzak, R.,
763 Moghaddam, M., 2012. AirMOSS: An airborne P-band SAR to measure root-zone
764 soil moisture. *IEEE Natl. Radar Conf. - Proc.* 0693–0698.
765 <https://doi.org/10.1109/RADAR.2012.6212227>
766 Collins, D.B.G., Bras, R.L., 2007. Plant rooting strategies in water-limited ecosystems.
767 *Water Resour. Res.* 43, 1–10. <https://doi.org/10.1029/2006WR005541>
768 Crow, W.T., Han, E., Ryu, D., Hain, C.R., Anderson, M.C., 2017. Estimating annual
769 water storage variations in medium-scale (2000-10000km²) basins using
770 microwave-based soil moisture retrievals. *Hydrol. Earth Syst. Sci.* 21, 1849–1862.
771 <https://doi.org/10.5194/hess-21-1849-2017>
772 Dawson, T.E., Pate, J.S., 1996. Seasonal water uptake and movement in root systems
773 of Australian phraeatophytic plants of dimorphic root morphology: A stable isotope
774 investigation. *Oecologia* 107, 13–20. <https://doi.org/10.1007/BF00582230>
775 Denissen, J.M.C., Teuling, A.J., Reichstein, M., Orth, R., 2020. Critical Soil Moisture
776 Derived From Satellite Observations Over Europe. *J. Geophys. Res. Atmos.* 125.
777 <https://doi.org/10.1029/2019JD031672>
778 Dong, J., Akbar, R., Gianotti, D.J.S., Feldman, A.F., Crow, W.T., Entekhabi, D., 2022.
779 Can Surface Soil Moisture Information Identify Evapotranspiration Regime

780 Transitions? *Geophys. Res. Lett.* e2021GL097697.

781 Dong, J., Crow, W.T., 2019. L-band remote-sensing increases sampled levels of global
782 soil moisture-air temperature coupling strength. *Remote Sens. Environ.* 220, 51–
783 58. <https://doi.org/10.1016/j.rse.2018.10.024>

784 Dong, J., Dirmeyer, P.A., Lei, F., Anderson, M.C., Holmes, T.R.H., Hain, C., Crow,
785 W.T., 2020. Soil Evaporation Stress Determines Soil Moisture-Evapotranspiration
786 Coupling Strength in Land Surface Modeling. *Geophys. Res. Lett.* 47, 1–11.
787 <https://doi.org/10.1029/2020GL090391>

788 Ehleringer, J.R., Dawson, T.E., 1992. Water uptake by plants: perspectives from stable
789 isotope composition. *Plant, Cell Environ.* [https://doi.org/10.1111/j.1365-](https://doi.org/10.1111/j.1365-3040.1992.tb01657.x)
790 [3040.1992.tb01657.x](https://doi.org/10.1111/j.1365-3040.1992.tb01657.x)

791 Entekhabi, D., Njoku, E.G., O'Neill, P.E., Kellogg, K.H., Crow, W.T., Edelstein, W.N.,
792 Entin, J.K., Goodman, S.D., Jackson, T.J., Johnson, J., Kimball, J., Piepmeier, J.R.,
793 Koster, R.D., Martin, N., McDonald, K.C., Moghaddam, M., Moran, S., Reichle, R.,
794 Shi, J.C., Spencer, M.W., Thurman, S.W., Tsang, L., Van Zyl, J., 2010. The Soil
795 Moisture Active Passive (SMAP) Mission. *Proc. IEEE* 98, 704–716.
796 <https://doi.org/10.1109/JPROC.2010.2043918>

797 Escorihuela, M.J., Chanzy, A., Wigneron, J.P., Kerr, Y.H., 2010. Effective soil moisture
798 sampling depth of L-band radiometry: A case study. *Remote Sens. Environ.* 114,
799 995–1001. <https://doi.org/10.1016/j.rse.2009.12.011>

800 Fan, Y., Miguez-Macho, G., Jobbágy, E.G., Jackson, R.B., Otero-Casal, C., 2017.
801 Hydrologic regulation of plant rooting depth. *Proc. Natl. Acad. Sci. U. S. A.* 114,
802 10572–10577. <https://doi.org/10.1073/pnas.1712381114>

803 Farahmand, A., Reager, J.T., Madani, N., 2021. Drought Cascade in the Terrestrial
804 Water Cycle: Evidence From Remote Sensing. *Geophys. Res. Lett.* 48, 1–10.
805 <https://doi.org/10.1029/2021GL093482>

806 Fatichi, S., Or, D., Walko, R., Vereecken, H., Young, M.H., Ghezzehei, T.A., Hengl, T.,
807 Kollet, S., Agam, N., Avissar, R., 2020. Soil structure is an important omission in
808 Earth System Models. *Nat. Commun.* 11, 1–11. [https://doi.org/10.1038/s41467-](https://doi.org/10.1038/s41467-020-14411-z)
809 [020-14411-z](https://doi.org/10.1038/s41467-020-14411-z)

810 Fatichi, S., Pappas, C., 2017. Constrained variability of modeled T:ET ratio across
811 biomes. *Geophys. Res. Lett.* 44, 6795–6803.
812 <https://doi.org/10.1002/2017GL074041>.Received

813 Feldman, A.F., Akbar, R., Entekhabi, D., 2018a. Characterization of Higher-Order
814 Scattering from Vegetation with SMAP Measurements. *Remote Sens. Environ.* 219,
815 324–338.

816 Feldman, A.F., Chaparro, D., Entekhabi, D., 2021. Error Propagation in Microwave Soil
817 Moisture and Vegetation Optical Depth Retrievals. *IEEE J. Sel. Top. Appl. Earth*
818 *Obs. Remote Sens.* 14, 11311–11323.

819 Feldman, A.F., Gianotti, D.J.S., Dong, J., Akbar, R., Crow, W.T., McColl, K.A., Konings,
820 A.G., Nippert, J.B., Tumber-Dávila, S.J., Holbrook, N.M., Rockwell, F.E., Scott,
821 R.L., Reichle, R.H., Chatterjee, A., Joiner, J., Poulter, B., Entekhabi, D., 2023.
822 Dataset: Remotely sensed soil moisture can capture dynamics relevant to plant
823 water uptake (Version 1) [Data set]. Zenodo.
824 <https://doi.org/10.5281/zenodo.7527459>. Zenodo.

825 Feldman, A.F., Gianotti, D.J.S., Trigo, I.F., Salvucci, G.D., Entekhabi, D., 2022.

826 Observed Landscape Responsiveness to Climate Forcing. *Water Resour. Res.* 58,
827 e2021WR030316.

828 Feldman, A.F., Short Gianotti, D.J., Konings, A.G., McColl, K.A., Akbar, R., Salvucci,
829 G.D., Entekhabi, D., 2018b. Moisture pulse-reserve in the soil-plant continuum
830 observed across biomes. *Nat. Plants* 4, 1026–1033.
831 <https://doi.org/10.1038/s41477-018-0304-9>

832 Fluhrer, A., Jagdhuber, T., Tabatabaeenejad, A., Alemohammad, H., Montzka, C.,
833 Friedl, P., Forootan, E., Kunstmann, H., 2022. Remote Sensing of Complex
834 Permittivity and Penetration Depth of Soils Using P-Band SAR Polarimetry. *Remote*
835 *Sens.* 14. <https://doi.org/10.3390/rs14122755>

836 Ford, T.W., Harris, E., Quiring, S.M., 2014. Estimating root zone soil moisture using
837 near-surface observations from SMOS. *Hydrol. Earth Syst. Sci.* 18, 139–154.
838 <https://doi.org/10.5194/hess-18-139-2014>

839 Garrison, J.L., Piepmeier, J.R., Shah, R., Vega, M.A., Spencer, D.A., Banting, R.,
840 Firman, C.M., Nold, B., Larsen, K., Bindlish, R., 2019. SNOOPI: A Technology
841 Validation Mission for P-band Reflectometry using Signals of Opportunity. *IEEE Int.*
842 *Geosci. Remote Sens. Symp.* 5082–5085.

843 Good, S.P., Caylor, K.K., 2011. Climatological determinants of woody cover in Africa.
844 *Proc. Natl. Acad. Sci. U. S. A.* 108, 4902–4907.
845 <https://doi.org/10.1073/pnas.1013100108>

846 Good, S.P., Noone, D., Bowen, G., 2015. Hydrologic connectivity constrains partitioning
847 of global terrestrial water fluxes. *Science* (80-). 349, 175–177.
848 <https://doi.org/10.1126/science.aaa5931>

849 Haghighi, E., Shahraeeni, E., Lehmann, P., Or, D., 2013. Evaporation rates across a
850 convective air boundary layer are dominated by diffusion. *Water Resour. Res.* 49,
851 1602–1610. <https://doi.org/10.1002/wrcr.20166>

852 Hirmas, D.R., Giménez, D., Nemes, A., Kerry, R., Brunzell, N.A., Wilson, C.J., 2018.
853 Climate-induced changes in continental-scale soil macroporosity may intensify
854 water cycle. *Nature*.

855 Huffman, G., 2015. GPM Level 3 IMERG Final Run Half Hourly 0.1 × 0.1 Degree
856 Precipitation, version 05 (Goddard Space Flight Center Distributed Active Archive
857 Center (GSFC DAAC), 2015).

858 Ichii, K., Hashimoto, H., White, M.A., Potter, C., Huttyra, L.R., Huete, A.R., Myneni, R.B.,
859 Nemani, R.R., 2007. Constraining rooting depths in tropical rainforests using
860 satellite data and ecosystem modeling for accurate simulation of gross primary
861 production seasonality. *Glob. Chang. Biol.* 13, 67–77.
862 <https://doi.org/10.1111/j.1365-2486.2006.01277.x>

863 Jackson, R.B., Canadell, J., Ehleringer, J.R., Mooney, H.A., Sala, O.E., Schulze, E.D.,
864 1996. A global analysis of root distributions for terrestrial biomes. *Oecologia* 108,
865 389–411. <https://doi.org/10.1007/BF00333714>

866 Jackson, T.J., Schmugge, T.J., O'Neill, P., 1984. Passive microwave remote sensing of
867 soil moisture from an aircraft platform. *Remote Sens. Environ.* 14, 135–151.
868 [https://doi.org/10.1016/0034-4257\(84\)90011-7](https://doi.org/10.1016/0034-4257(84)90011-7)

869 Jasechko, S., Sharp, Z.D., Gibson, J.J., Birks, S.J., Yi, Y., Fawcett, P.J., 2013.
870 Terrestrial water fluxes dominated by transpiration. *Nature* 496, 347–350.
871 <https://doi.org/10.1038/nature11983>

872 Jiang, P., Wang, H., Meinzer, F.C., Kou, L., Dai, X., Fu, X., 2020. Linking reliance on
873 deep soil water to resource economy strategies and abundance among coexisting
874 understorey shrub species in subtropical pine plantations. *New Phytol.* 225, 222–
875 233. <https://doi.org/10.1111/nph.16027>

876 Jobbágy, E.G., Jackson, R.B., 2001. The distribution of soil nutrients with depth: Global
877 patterns and the imprint of plants. *Biogeochemistry* 53, 51–77.
878 <https://doi.org/10.1023/A:1010760720215>

879 Jones, H.G., 2014. *Plants and Microclimate: A Quantitative Approach to Environmental*
880 *Plant Physiology*, 3rd ed. Cambridge University Press, Cambridge, UK.

881 Katul, G.G., Oren, R., Manzoni, S., Higgins, C., Parlange, M.B., 2012.
882 *Evapotranspiration: A process driving mass transport and energy exchange in the*
883 *soil-plant-atmosphere-climate system.* *Rev. Geophys.* 50.
884 <https://doi.org/10.1029/2011RG000366>

885 Katul, G.G., Siqueira, M.B., 2010. Biotic and abiotic factors act in coordination to amplify
886 hydraulic redistribution and lift. *New Phytol.* 187, 3–6.
887 <https://doi.org/10.1111/j.1469-8137.2010.03306.x>

888 Kerr, Y., Waldteufel, P., Wigneron, J.-P., Delwart, S., Cabot, F., Boutin, J., Escorihuela,
889 M.J., Font, J., Reul, N., Gruhier, C., Juglea, S.E., Drinkwater, M.R., Achim HReul,
890 N., Boutin, J., Gruhier, C., Juglea, S.E., Drinkwater, M.R., Hahne, A., Neira, M.M.-,
891 Mecklenburg, S., 2010. The SMOS Mission: New Tool for Monitoring Key Elements
892 of the Global Water Cycle. *Proc. IEEE* 98, 666–687.

893 Konings, A.G., Entekhabi, D., Moghaddam, M., Saatchi, S.S., 2014. The Effect of a
894 Variable Soil Moisture Profile on P-band Backscatter Estimation. *IEEE Trans.*
895 *Geosci. Remote Sens.* 52, 6315–6325.

896 Konings, A.G., Williams, A.P., Gentine, P., 2017. Sensitivity of grassland productivity to
897 aridity controlled by stomatal and xylem regulation. *Nat. Geosci.* 10, 284–288.
898 <https://doi.org/10.1038/ngeo2903>

899 Koster, R.D., Schubert, S.D., Wang, H., Mahanama, S.P., Deangelis, A.M., 2019. Flash
900 drought as captured by reanalysis data: Disentangling the contributions of
901 precipitation deficit and excess evapotranspiration. *J. Hydrometeorol.* 20, 1241–
902 1258. <https://doi.org/10.1175/JHM-D-18-0242.1>

903 Koster, R.D., Suarez, M.J., 2001. Soil moisture memory in climate models. *J.*
904 *Hydrometeorol.* 2, 558–570. [https://doi.org/10.1175/1525-](https://doi.org/10.1175/1525-7541(2001)002<0558:SMMICM>2.0.CO;2)
905 [7541\(2001\)002<0558:SMMICM>2.0.CO;2](https://doi.org/10.1175/1525-7541(2001)002<0558:SMMICM>2.0.CO;2)

906 Kramer, P.J., Boyer, J.S., 1995. *Water Relations of Plants and Soils.* Academic Press.

907 Kulmatiski, A., Beard, K.H., 2013. Root niche partitioning among grasses, saplings, and
908 trees measured using a tracer technique. *Oecologia* 171, 25–37.
909 <https://doi.org/10.1007/s00442-012-2390-0>

910 Kulmatiski, A., Beard, K.H., Verweij, R.J.T., February, E.C., 2010. A depth-controlled
911 tracer technique measures vertical, horizontal and temporal patterns of water use
912 by trees and grasses in a subtropical savanna. *New Phytol.* 188, 199–209.
913 <https://doi.org/10.1111/j.1469-8137.2010.03338.x>

914 Kurum, M., Lang, R.H., O'Neill, P.E., Joseph, A.T., Jackson, T.J., Cosh, M.H., 2011. A
915 first-order radiative transfer model for microwave radiometry of forest canopies at L-
916 band. *IEEE Trans. Geosci. Remote Sens.* 49, 3167–3179.
917 <https://doi.org/10.1109/TGRS.2010.2091139>

918 Landsberg, J.J., Fowkes, N.D., 1978. Water Movement Through Plant Roots. *Ann. Bot.*
919 42, 493–508.

920 Le Roux, X., Bariac, T., Mariotti, A., 1995. Spatial Partitioning of the Soil Water
921 Resource between Grass and Shrub Components in a West African Humid
922 Savanna. *Oecologia* 104, 147–155.

923 Lehmann, P., Assouline, S., Or, D., 2008. Characteristic lengths affecting evaporative
924 drying of porous media. *Phys. Rev. E - Stat. Nonlinear, Soft Matter Phys.* 77, 1–16.
925 <https://doi.org/10.1103/PhysRevE.77.056309>

926 Li, F., Crow, W.T., Kustas, W.P., 2010. Towards the estimation root-zone soil moisture
927 via the simultaneous assimilation of thermal and microwave soil moisture retrievals.
928 *Adv. Water Resour.* 33, 201–214. <https://doi.org/10.1016/j.advwatres.2009.11.007>

929 Li, W., Migliavacca, M., Forkel, M., Walther, S., Reichstein, M., Orth, R., 2021.
930 Revisiting Global Vegetation Controls Using Multi-Layer Soil Moisture. *Geophys.*
931 *Res. Lett.* 48. <https://doi.org/10.1029/2021GL092856>

932 Liu, L., Gudmundsson, L., Hauser, M., Qin, D., Li, S., Seneviratne, S.I., 2020. Soil
933 moisture dominates dryness stress on ecosystem production globally. *Nat.*
934 *Commun.* 11, 4892. <https://doi.org/10.1038/s41467-020-18631-1>

935 Liu, P.W., Judge, J., DeRoo, R.D., England, A.W., Bongiovanni, T., Luke, A., 2016.
936 Dominant backscattering mechanisms at L-band during dynamic soil moisture
937 conditions for sandy soils. *Remote Sens. Environ.* 178, 104–112.
938 <https://doi.org/10.1016/j.rse.2016.02.062>

939 Lv, S., Zeng, Y., Wen, J., Zhao, H., Su, Z., 2018. Estimation of penetration depth from
940 soil effective temperature in microwave radiometry. *Remote Sens.* 10, 1–19.
941 <https://doi.org/10.3390/rs10040519>

942 Macelloni, G., Paloscia, S., Pampaloni, P., Santi, E., Tedesco, M., 2003. Microwave
943 radiometric measurements of soil moisture in Italy. *Hydrol. Earth Syst. Sci.* 7, 937–
944 948. <https://doi.org/10.5194/hess-7-937-2003>

945 Mätzler, C., 1998. Microwave Permittivity of Dry Sand. *IEEE Trans. Geosci. Remote*
946 *Sens.* 36, 317–319. <https://doi.org/10.1109/36.655342>

947 McColl, K.A., Alemohammad, S.H., Akbar, R., Konings, A.G., Yueh, S., Entekhabi, D.,
948 2017. The global distribution and dynamics of surface soil moisture. *Nat. Geosci.*
949 10, 100–104. <https://doi.org/10.1038/ngeo2868>

950 McCormick, E.L., Dralle, D.N., Hahm, W.J., Tune, A.K., Schmidt, L.M., Chadwick, K.D.,
951 Rempe, D.M., 2021. Widespread woody plant use of water stored in bedrock.
952 *Nature* 597, 225–229. <https://doi.org/10.1038/s41586-021-03761-3>

953 Miguez-Macho, G., Fan, Y., 2021. Spatiotemporal origin of soil water taken up by
954 vegetation. *Nature*.

955 Moghaddam, M., Saatchi, S., Cuenca, R.H., 2000. Estimating subcanopy soil moisture
956 with radar. *J. Geophys. Res. Atmos.* 105, 14899–14911.
957 <https://doi.org/10.1029/2000JD900058>

958 Mueller, B., Seneviratne, S.I., 2012. Hot days induced by precipitation deficits at the
959 global scale. *Proc. Natl. Acad. Sci. U. S. A.* 109, 12398–12403.
960 <https://doi.org/10.1073/pnas.1204330109>

961 Nadezhdina, N., David, T.S., David, J.S., Ferreira, M.I., Dohnal, M., Tesar, M., Gartner,
962 K., Leitgeb, E., Nadezhdin, V., Cermak, J., Jimenez, M.S., Morales, D., 2010. Trees
963 never rest: the multiple facets of hydraulic redistribution. *Ecohydrology* 3, 431–444.

964 <https://doi.org/10.1002/eco>
965 Nepstad, D.C., de Carvalho, C.R., Davidson, E.A., Jipp, P.H., Lefebvre, P.A., Negreiros,
966 G.H., da Silva, E.D., Stone, T.A., Trumbore, S.E., Vieira, S., 1994. The role of deep
967 roots in the hydrological and carbon cycles of Amazonian forests and pastures.
968 *Nature* 372, 666–669. <https://doi.org/10.1038/372666a0>
969 Newton, R.W., Black, Q.R., Mankanvand, S., Blanchard, A.J., Jean, B.R., 1982. Soil
970 Moisture Information and Thermal Microwave Emission. *IEEE Trans. Geosci.*
971 *Remote Sens. GE-20*, 275–281. <https://doi.org/10.1109/TGRS.1982.350443>
972 Nippert, J.B., Holdo, R.M., 2015. Challenging the maximum rooting depth paradigm in
973 grasslands and savannas. *Funct. Ecol.* 29, 739–745. [https://doi.org/10.1111/1365-](https://doi.org/10.1111/1365-2435.12390)
974 [2435.12390](https://doi.org/10.1111/1365-2435.12390)
975 Nippert, J.B., Wieme, R.A., Ocheltree, T.W., Craine, J.M., 2012. Root characteristics of
976 C4 grasses limit reliance on deep soil water in tallgrass prairie. *Plant Soil* 355, 385–
977 394. <https://doi.org/10.1007/s11104-011-1112-4>
978 Njoku, E.G., Entekhabi, D., 1996. Passive microwave remote sensing of soil moisture.
979 *J. Hydrol.* 184, 101–129. [https://doi.org/10.1016/0022-1694\(95\)02970-2](https://doi.org/10.1016/0022-1694(95)02970-2)
980 Njoku, E.G., Jackson, T.J., Lakshmi, V., Chan, T.K., Nghiem, S. V., 2003. Soil moisture
981 retrieval from AMSR-E. *IEEE Trans. Geosci. Remote Sens.* 41, 215–228.
982 <https://doi.org/10.1109/TGRS.2002.808243>
983 Njoku, E.G., Kong, J.-A., 1977. Theory for passive microwave remote sensing of near-
984 surface soil moisture. *J. Geophys. Res.* 82, 3108.
985 <https://doi.org/10.1029/JB082i020p03108>
986 Njoku, E.G., O'Neill, P.E., 1982. Multifrequency Microwave Radiometer Measurements
987 of Soil Moisture. *IEEE Trans. Geosci. Remote Sens.* 20, 468–475.
988 <https://doi.org/10.1109/igarss.1990.688877>
989 Ogle, K., Wolpert, R.L., Reynolds, J.F., 2004. Reconstructing plant root area and water
990 uptake profiles. *Ecology* 85, 1967–1978. <https://doi.org/10.1890/03-0346>
991 Or, D., 2020. The Tyranny of Small Scales—On Representing Soil Processes in Global
992 Land Surface Models. *Water Resour. Res.* 56.
993 <https://doi.org/10.1029/2019WR024846>
994 Or, D., Lehmann, P., 2019. Surface Evaporative Capacitance: How Soil Type and
995 Rainfall Characteristics Affect Global-Scale Surface Evaporation. *Water Resour.*
996 *Res.* 55, 519–539. <https://doi.org/10.1029/2018WR024050>
997 Owe, M., Van De Griend, A.A., 1998. Comparison of soil moisture penetration depths
998 for several bare soils at two microwave frequencies and implications for remote
999 sensing. *Water Resour. Res.* 34, 2319–2327. <https://doi.org/10.1029/98WR01469>
1000 Pampaloni, P., Paloscia, S., Chiarantini, L., Coppo, P., Gagliani, S., Luzi, G., 1990.
1001 Sampling depth of soil moisture content by radiometric measurement at 21 cm
1002 wavelength: Some experimental results. *Int. J. Remote Sens.* 11, 1085–1092.
1003 <https://doi.org/10.1080/01431169008955080>
1004 Peng, J., Albergel, C., Balenzano, A., Brocca, L., Cartus, O., Cosh, M.H., Crow, W.T.,
1005 Dabrowska-Zielinska, K., Dadson, S., Davidson, M.W.J., de Rosnay, P., Dorigo,
1006 W., Gruber, A., Hagemann, S., Hirschi, M., Kerr, Y.H., Lovergine, F., Mahecha,
1007 M.D., Marzahn, P., Mattia, F., Musial, J.P., Preuschmann, S., Reichle, R.H.,
1008 Satalino, G., Silgram, M., van Bodegom, P.M., Verhoest, N.E.C., Wagner, W.,
1009 Walker, J.P., Wegmüller, U., Loew, A., 2021. A roadmap for high-resolution satellite

1010 soil moisture applications – confronting product characteristics with user
1011 requirements. *Remote Sens. Environ.* 252.
1012 <https://doi.org/10.1016/j.rse.2020.112162>

1013 Peng, J., Loew, A., Merlin, O., Verhoest, N.E.C., 2017. A review of spatial downscaling
1014 of satellite remotely sensed soil moisture. *Rev. Geophys.* 55, 341–366.
1015 <https://doi.org/10.1029/88EO01108>

1016 Phillips, M.L., Mcnellis, B.E., Howell, A., Lauria, C.M., Belnap, J., Reed, S.C., 2022.
1017 Biocrusts mediate a new mechanism for land degradation Under a Changing
1018 Climate. *Nat. Clim. Chang.* 12, 71–76.

1019 Prechsl, U.E., Burri, S., Gilgen, A.K., Kahmen, A., Buchmann, N., 2015. No shift to a
1020 deeper water uptake depth in response to summer drought of two lowland and sub-
1021 alpine C3-grasslands in Switzerland. *Oecologia* 177, 97–111.
1022 <https://doi.org/10.1007/s00442-014-3092-6>

1023 Purdy, A.J., Fisher, J.B., Goulden, M.L., Colliander, A., Halverson, G., Tu, K.,
1024 Famiglietti, J.S., 2018. SMAP soil moisture improves global evapotranspiration.
1025 *Remote Sens. Environ.* 219, 1–14.
1026 <https://doi.org/https://doi.org/10.1016/j.rse.2018.09.023>

1027 Qiu, J., Crow, W.T., Nearing, G.S., 2016. The impact of vertical measurement depth on
1028 the information content of soil moisture for latent heat flux estimation. *J.*
1029 *Hydrometeorol.* 17, 2419–2430. <https://doi.org/10.1175/JHM-D-16-0044.1>

1030 Qiu, J., Crow, W.T., Nearing, G.S., Mo, X., Liu, S., 2014. The impact of vertical
1031 measurement depth on the information content of soil moisture times series data.
1032 *Geophys. Res. Lett.* 41, 4997–5004.
1033 <https://doi.org/10.1002/2014GL060017>.Received

1034 Quegan, S., Le Toan, T., Chave, J., Dall, J., Exbrayat, J.F., Minh, D.H.T., Lomas, M.,
1035 D’Alessandro, M.M., Paillou, P., Papathanassiou, K., Rocca, F., Saatchi, S., Scipal,
1036 K., Shugart, H., Smallman, T.L., Soja, M.J., Tebaldini, S., Ulander, L., Villard, L.,
1037 Williams, M., 2019. The European Space Agency BIOMASS mission: Measuring
1038 forest above-ground biomass from space. *Remote Sens. Environ.* 227, 44–60.
1039 <https://doi.org/10.1016/j.rse.2019.03.032>

1040 Rao, K.S., Chandra, G., Rao, P.V.N., 1988. STUDY ON PENETRATION DEPTH AND
1041 ITS DEPENDENCE ON FREQUENCY, SOIL MOISTURE, TEXTURE AND
1042 TEMPERATURE IN THE CONTEXT OF MICROWAVE REMOTE SENSING. *J.*
1043 *Indian Soc. Remote Sens.*

1044 Reichle, R.H., Liu, Q., Koster, R.D., Crow, W.T., 2019. Version 4 of the SMAP Level - 4
1045 Soil Moisture Algorithm and Data Product. *J. Adv. Model. Earth Syst.* 11, 3106–
1046 3130.

1047 Rodell, M., Famiglietti, J.S., 2001. An analysis of terrestrial water storage variations in
1048 Illinois with implications for the Gravity Recovery and Climate Experiment
1049 (GRACE). *Water Resour. Res.* 37, 1327–1339.
1050 <https://doi.org/10.1029/2000WR900306>

1051 Roth, L.E., Elachi, C., 1975. Coherent Electromagnetic Losses by Scattering from
1052 Volume Inhomogeneities. *IEEE Trans. Antennas Propag.* 674–675.

1053 Salvucci, G.D., 1997. Soil and moisture independent estimation of stage-two
1054 evaporation from potential evaporation and albedo or surface temperature
1055 approximately preserve similarity during simultaneous. *Water Resour. Res.* 33,

1056 111–122. <https://doi.org/10.1029/96WR02858>

1057 Santanello, J.A., Lawston, P., Kumar, S., Dennis, E., 2019. Understanding the impacts
1058 of soil moisture initial conditions on NWP in the context of land-atmosphere
1059 coupling. *J. Hydrometeorol.* 20, 793–819. <https://doi.org/10.1175/JHM-D-18-0186.1>

1060 Schenk, H. Jochen, Jackson, R.B., 2002. Rooting depths, lateral root spreads and
1061 below-ground/above-ground allometries of plants in water-limited ecosystems. *J.*
1062 *Ecol.* 90, 480–494. <https://doi.org/10.1046/j.1365-2745.2002.00682.x>

1063 Schenk, H. J., Jackson, R.B., 2002. the Global Biogeography of Roots. *Ecol. Monogr.*
1064 72, 311–328. [https://doi.org/10.1890/0012-9615\(2002\)072\[0311:TGBOR\]2.0.CO;2](https://doi.org/10.1890/0012-9615(2002)072[0311:TGBOR]2.0.CO;2)

1065 Schimel, D., Pavlick, R., Fisher, J.B., Asner, G.P., Saatchi, S., Townsend, P., Miller, C.,
1066 Frankenberg, C., Hibbard, K., Cox, P., 2015. Observing terrestrial ecosystems and
1067 the carbon cycle from space. *Glob. Chang. Biol.* 21, 1762–1776.
1068 <https://doi.org/10.1111/gcb.12822>

1069 Schmugge, T.J., 1983. Remote Sensing of Soil Moisture: Recent Advances. *Adv. Sp.*
1070 *Res.* 21, 336–334. [https://doi.org/10.1016/0273-1177\(87\)90304-8](https://doi.org/10.1016/0273-1177(87)90304-8)

1071 Scott, C.A., Bastiaanssen, W.G.M., Ahmad, M.-D., 2003. Mapping Root Zone Soil
1072 Moisture Using Remotely Sensed Optical Imagery. *J. Irrig. Drain. Eng.* 129, 326–
1073 335. [https://doi.org/10.1061/\(asce\)0733-9437\(2003\)129:5\(326\)](https://doi.org/10.1061/(asce)0733-9437(2003)129:5(326))

1074 Scott, R.L., Biederman, J.A., 2019. Critical Zone Water Balance Over 13 Years in a
1075 Semiarid Savanna. *Water Resour. Res.* 55, 574–588.
1076 <https://doi.org/10.1029/2018WR023477>

1077 Sehgal, V., Gaur, N., Mohanty, B.P., 2021. Global Surface Soil Moisture Drydown
1078 Patterns. *Water Resour. Res.* 57, 1–26. <https://doi.org/10.1029/2020WR027588>

1079 Shen, X., Walker, J.P., Ye, N., Wu, X., Boopathi, N., Yeo, I.Y., Zhang, L., Zhu, L., 2021.
1080 Soil Moisture Retrieval Depth of P- And L-Band Radiometry: Predictions and
1081 Observations. *IEEE Trans. Geosci. Remote Sens.* 59, 6814–6822.
1082 <https://doi.org/10.1109/TGRS.2020.3026384>

1083 Short Gianotti, D.J., Akbar, R., Feldman, A.F., Salvucci, G.D., Entekhabi, D., 2020.
1084 Terrestrial Evaporation and Moisture Drainage in a Warmer Climate. *Geophys.*
1085 *Res. Lett.* 47, e2019GL086498. <https://doi.org/10.1029/2019GL086498>

1086 Short Gianotti, D.J., Salvucci, G.D., Akbar, R., McColl, K.A., Cuenca, R., Entekhabi, D.,
1087 2019. Landscape water storage and subsurface correlation from satellite surface
1088 soil moisture and precipitation observations. *Water Resour. Res.* 9111–9132.
1089 <https://doi.org/10.1029/2019wr025332>

1090 Stocker, B.D., Tumber-d, S.J., Konings, A.G., Anderson, M.B., Hain, C., Jackson, R.B.,
1091 2021. Global distribution of the rooting zone water storage capacity reflects plant
1092 adaptation to the environment 1–20.

1093 Taylor, C.M., De Jeu, R.A.M., Harris, P.P., Dorigo, W.A., Africa, W., 2012. Afternoon
1094 rain more likely over drier soils. *Nature* 489, 423–426.
1095 <https://doi.org/10.1038/nature11377>

1096 Tsang, L., Njoku, E., Kong, J.A., 1975. Microwave thermal emission from a stratified
1097 medium with nonuniform temperature distribution. *J. Appl. Phys.* 46, 5127–5133.
1098 <https://doi.org/10.1063/1.321571>

1099 Tumber-Dávila, S.J., Malhotra, A., 2020. Fast plants in deep water: introducing the
1100 whole-soil column perspective. *New Phytol.* 225, 7–9.
1101 <https://doi.org/10.1111/nph.16302>

1102 Tumber-Dávila, S.J., Schenk, H.J., Du, E., Jackson, R.B., 2022. Plant sizes and shapes
1103 above- and belowground and their interactions with climate. *New Phytol.*
1104 <https://doi.org/10.1111/nph.18031>

1105 Tuttle, S., Salvucci, G., 2016. Empirical evidence of contrasting soil moisture-
1106 precipitation feedbacks across the United States. *Science* (80-.). 352, 825–827.

1107 Ulaby, F.T., Long, D.G., 2014. *Microwave Radar and Radiometric Remote Sensing.*
1108 University of Michigan Press, Ann Arbor.

1109 Vereecken, H., Amelung, W., Bauke, S.L., Bogaen, H., Brüggemann, N., Montzka, C.,
1110 Vanderborght, J., Bechtold, M., Blöschl, G., Carminati, A., Javaux, M., Konings,
1111 A.G., 2022. Soil hydrology in the Earth system. *Nat. Rev. Earth Environ.*

1112 Wang-Erlandsson, L., Bastiaanssen, W.G.M., Gao, H., Jägermeyr, J., Senay, G.B., Van
1113 Dijk, A.I.J.M., Guerschman, J.P., Keys, P.W., Gordon, L.J., Savenije, H.H.G., 2016.
1114 Global root zone storage capacity from satellite-based evaporation. *Hydrol. Earth*
1115 *Syst. Sci.* 20, 1459–1481. <https://doi.org/10.5194/hess-20-1459-2016>

1116 Wang, J.R., 1987. Smooth Bare Fields and Sampling Depth. *IEEE Trans. Geosci.*
1117 *Remote Sens.* 5, 616–622.

1118 Werner, C., Meredith, L.K., Ladd, S.N., Ingrisch, J., Kübert, A., van Haren, J., Bahn, M.,
1119 Bailey, K., Bamberger, I., Beyer, M., Blomdahl, D., Byron, J., Daber, E., Deleeuw,
1120 J., Dippold, M.A., Fudyma, J., Gil-Loaiza, J., Honeker, L.K., Hu, J., Huang, J.,
1121 Klüpfel, T., Krechmer, J., Kreuzwieser, J., Kühnhammer, K., Lehmann, M.M.,
1122 Meeran, K., Misztal, P.K., Ng, W.R., Pfannerstill, E., Pugliese, G., Purser, G.,
1123 Roscioli, J., Shi, L., Tfaily, M., Williams, J., 2021. Ecosystem fluxes during drought
1124 and recovery in an experimental forest. *Science* (80-.). 374, 1514–1518.
1125 <https://doi.org/10.1126/science.abj6789>

1126 Wilheit, T.T., 1978. Radiative Transfer in a Plane Stratified Dielectric. *IEEE Trans.*
1127 *Geosci. Electron.* 16, 138–143. <https://doi.org/10.1109/TGE.1978.294577>

1128 Xiong, S., Muller, J.P., Li, G., 2017. The application of ALOS/PALSAR InSAR to
1129 measure subsurface penetration depths in deserts. *Remote Sens.* 9, 1–19.
1130 <https://doi.org/10.3390/rs9060638>

1131 Zhang, Z., Chatterjee, A., Ott, L., Reichle, R., Feldman, A.F., Poulter., B., 2022. Soil
1132 moisture controls on seasonal and interannual terrestrial carbon fluxes: Potential of
1133 directly inserting SMAP soil moisture into a carbon cycle model. *Remote Sens.* In
1134 Press.

1135 Zhou, S., Williams, A.P., Lintner, B.R., Berg, A.M., Zhang, Y., Keenan, T.F., Cook, B.I.,
1136 Hagemann, S., Seneviratne, S.I., Gentile, P., 2021. Soil moisture–atmosphere
1137 feedbacks mitigate declining water availability in drylands. *Nat. Clim. Chang.* 11,
1138 38–44. <https://doi.org/10.1038/s41558-020-00945-z>

1139 Zwieback, S., Bosch, D.D., Cosh, M.H., Starks, P.J., Berg, A., 2019. Vegetation–soil
1140 moisture coupling metrics from dual-polarization microwave radiometry using
1141 regularization. *Remote Sens. Environ.* 231, 111257.
1142 <https://doi.org/10.1016/j.rse.2019.111257>

1143 Zwieback, S., Hensley, S., Hajnsek, I., 2015. Assessment of soil moisture effects on L-
1144 band radar interferometry. *Remote Sens. Environ.* 164, 77–89.
1145 <https://doi.org/10.1016/j.rse.2015.04.012>

1146
1147

1148

1149 **References from Supporting Information**

- 1150 Asbjornsen, H., Mora, G., Helmers, M.J., 2007. Variation in water uptake dynamics
1151 among contrasting agricultural and native plant communities in the Midwestern
1152 U.S. *Agric. Ecosyst. Environ.* 121, 343–356.
- 1153 Asbjornsen, H., Shepherd, G., Helmers, M., Mora, G., 2008. Seasonal patterns in depth
1154 of water uptake under contrasting annual and perennial systems in the Corn Belt
1155 Region of the Midwestern U.S. *Plant Soil* 308, 69–92.
1156 <https://doi.org/10.1007/s11104-008-9607-3>
- 1157 Bachmann, D., Gockele, A., Ravenek, J.M., Roscher, C., Strecker, T., Weigelt, A.,
1158 Buchmann, N., 2015. No evidence of complementary water use along a plant
1159 species richness gradient in temperate experimental grasslands. *PLoS One* 10, 1–
1160 14. <https://doi.org/10.1371/journal.pone.0116367>
- 1161 Brinkmann, N., Eugster, W., Buchmann, N., Kahmen, A., 2019. Species-specific
1162 differences in water uptake depth of mature temperate trees vary with water
1163 availability in the soil. *Plant Biol.* 21, 71–81. <https://doi.org/10.1111/plb.12907>
- 1164 Brooks, J.R., Meinzer, F.C., Coulombe, R., Gregg, J., 2002. Hydraulic redistribution of
1165 soil water during summer drought in two contrasting Pacific Northwest coniferous
1166 forests. *Tree Physiol.* 22, 1107–1117. [https://doi.org/10.1093/treephys/22.15-](https://doi.org/10.1093/treephys/22.15-16.1107)
1167 [16.1107](https://doi.org/10.1093/treephys/22.15-16.1107)
- 1168 Case, M.F., Nippert, J.B., Holdo, R.M., Staver, A.C., 2020. Root-niche separation
1169 between savanna trees and grasses is greater on sandier soils. *J. Ecol.* 108,
1170 2298–2308. <https://doi.org/10.1111/1365-2745.13475>
- 1171 Chimner, R.A., Cooper, D.J., 2004. Using stable oxygen isotopes to quantify the water
1172 source used for transpiration by native shrubs in the San Luis Valley, Colorado
1173 U.S.A. *Plant Soil* 260, 225–236.
1174 <https://doi.org/10.1023/B:PLSO.0000030190.70085.e9>
- 1175 Clément, C., Sleiderink, J., Svane, S.F., Smith, A.G., Diamantopoulos, E., Desbrøll,
1176 D.B., Thorup-Kristensen, K., 2022. Comparing the deep root growth and water
1177 uptake of intermediate wheatgrass (Kernza®) to alfalfa. *Plant Soil* 472, 369–390.
1178 <https://doi.org/10.1007/s11104-021-05248-6>
- 1179 Dai, Y., Zheng, X.-J., Tang, L.-S., Li, Y., 2015. Stable oxygen isotopes reveal distinct
1180 water use patterns of two *Haloxylon* species in the Gurbantonggut Desert. *Plant*
1181 *Soil* 389, 73–87. [https://doi.org/10.1007/s](https://doi.org/10.1007/s11104-021-05248-6)
- 1182 Eggemeyer, K.D., Awada, T., Harvey, F.E., Wedin, D.A., Zhou, X., Zanner, C.W., 2009.
1183 Seasonal changes in depth of water uptake for encroaching trees *Juniperus*
1184 *virginiana* and *Pinus ponderosa* and two dominant C4 grasses in a semiarid
1185 grassland. *Tree Physiol.* 29, 157–169. <https://doi.org/10.1093/treephys/tpn019>
- 1186 Ellsworth, P.Z., Sternberg, L.S.L., 2015. Seasonal water use by deciduous and
1187 evergreen woody species in a scrub community is based on water availability and
1188 root distribution. *Ecohydrology* 8, 538–551. <https://doi.org/10.1002/eco.1523>
- 1189 Goldsmith, G.R., Muñoz-Villers, L.E., Holwerda, F., McDonnell, J.J., Asbjornsen, H.,
1190 Dawson, T.E., 2012. Stable isotopes reveal linkages among ecohydrological
1191 processes in a seasonally dry tropical montane cloud forest. *Ecohydrology* 5, 779–
1192 790. <https://doi.org/10.1002/eco.268>

1193 Hahn, M., Jacobs, S.R., Breuer, L., Rufino, M.C., Windhorst, D., 2021. Variability in tree
1194 water uptake determined with stable water isotopes in an African tropical montane
1195 forest. *Ecohydrology* 14, 1–14. <https://doi.org/10.1002/eco.2278>

1196 Hartsough, P., Poulson, S.R., Biondi, F., Estrada, I.G., 2008. Stable isotope
1197 characterization of the ecohydrological cycle at a tropical treeline site. *Arctic,*
1198 *Antarct. Alp. Res.* 40, 343–354. [https://doi.org/10.1657/1523-0430\(06-117\)\[HARTSOUGH\]2.0.CO;2](https://doi.org/10.1657/1523-0430(06-117)[HARTSOUGH]2.0.CO;2)

1200 Hoekstra, N.J., Finn, J.A., Hofer, D., Lüscher, A., 2014. The effect of drought and
1201 interspecific interactions on depth of water uptake in deep- and shallow-rooting
1202 grassland species as determined by $\delta^{18}\text{O}$ natural abundance. *Biogeosciences* 11,
1203 4493–4506. <https://doi.org/10.5194/bg-11-4493-2014>

1204 Jackson, P.C., Cavelier, J., Goldstein, G., Meinzer, F.C., Holbrook, N.M., 1995.
1205 Partitioning of water resources among plants of a lowland tropical forest. *Oecologia*
1206 101, 197–203. <https://doi.org/10.1007/BF00317284>

1207 Jackson, P.C., Meinzer, F.C., Bustamante, M., Goldstein, G., Franco, A., Rundel, P.W.,
1208 Caldas, L., Iglar, E., Causin, F., 1999. Partitioning of soil water among tree species
1209 in a Brazilian Cerrado ecosystem. *Tree Physiol.* 19, 717–724.
1210 <https://doi.org/10.1093/treephys/19.11.717>

1211 Kulmatiski, A., Beard, K.H., 2013. Root niche partitioning among grasses, saplings, and
1212 trees measured using a tracer technique. *Oecologia* 171, 25–37.
1213 <https://doi.org/10.1007/s00442-012-2390-0>

1214 Kulmatiski, A., Beard, K.H., Verweij, R.J.T., February, E.C., 2010. A depth-controlled
1215 tracer technique measures vertical, horizontal and temporal patterns of water use
1216 by trees and grasses in a subtropical savanna. *New Phytol.* 188, 199–209.
1217 <https://doi.org/10.1111/j.1469-8137.2010.03338.x>

1218 Le Roux, X., Bariac, T., Mariotti, A., 1995. Spatial Partitioning of the Soil Water
1219 Resource between Grass and Shrub Components in a West African Humid
1220 Savanna. *Oecologia* 104, 147–155.

1221 Li, S.G., Tsujimura, M., Sugimoto, A., Sasaki, L., Yamanaka, T., Davaa, G.,
1222 Oyunbaatar, D., Sugita, M., 2006. Seasonal variation in oxygen isotope
1223 composition of waters for a montane larch forest in Mongolia. *Trees - Struct. Funct.*
1224 20, 122–130. <https://doi.org/10.1007/s00468-005-0019-1>

1225 Liu, Wenjie, Liu, Wenyao, Li, P., Duan, W., Li, H., 2010. Dry season water uptake by
1226 two dominant canopy tree species in a tropical seasonal rainforest of
1227 Xishuangbanna, SW China. *Agric. For. Meteorol.* 150, 380–388.
1228 <https://doi.org/10.1016/j.agrformet.2009.12.006>

1229 Liu, Y., Xu, Z., Duffy, R., Chen, W., An, S., Liu, S., Liu, F., 2011. Analyzing relationships
1230 among water uptake patterns, rootlet biomass distribution and soil water content
1231 profile in a subalpine shrubland using water isotopes. *Eur. J. Soil Biol.* 47, 380–
1232 386. <https://doi.org/10.1016/j.ejsobi.2011.07.012>

1233 Liu, Y., Zhang, X., Zhao, S., Ma, H., Qi, G., Guo, S., 2019. The depth of water taken up
1234 by Walnut trees during different phenological stages in an irrigated arid hilly area in
1235 the Taihang Mountains. *Forests* 10. <https://doi.org/10.3390/f10020121>

1236 Ma, Y., Song, X., 2018. Seasonal variations in water uptake patterns of winter wheat
1237 under different irrigation and fertilization treatments. *Water (Switzerland)* 10.
1238 <https://doi.org/10.3390/w10111633>

1239 Meinzer, F.C., Luis, J., Goldstein, G., Holbrook, N.M., Cavelier, J., Wright, S.J., 1999.
1240 Partitioning of soil water among canopy trees in a seasonally dry tropical forest.
1241 *Oecologia* 293–301. <https://doi.org/10.1007/s004420050931>
1242 Moreira, M.Z., Sternberg, L. da S.L., Nepstad, D.C., 2000. Vertical patterns of soil water
1243 uptake by plants in a primary forest and an abandoned pasture in the eastern
1244 Amazon: An isotopic approach. *Plant Soil* 222, 95–107.
1245 <https://doi.org/10.1023/a:1004773217189>
1246 Muñoz-Villers, L.E., Geris, J., Alvarado-Barrientos, M.S., Holwerda, F., Dawson, T.,
1247 2020. Coffee and shade trees show complementary use of soil water in a
1248 traditional agroforestry ecosystem. *Hydrol. Earth Syst. Sci.* 24, 1649–1668.
1249 <https://doi.org/10.5194/hess-24-1649-2020>
1250 Nippert, J.B., Knapp, A.K., 2007. Linking water uptake with rooting patterns in grassland
1251 species. *Oecologia* 153, 261–272. <https://doi.org/10.1007/s00442-007-0745-8>
1252 Ogle, K., Wolpert, R.L., Reynolds, J.F., 2004. Reconstructing plant root area and water
1253 uptake profiles. *Ecology* 85, 1967–1978. <https://doi.org/10.1890/03-0346>
1254 Ohte, N., Koba, K., Yoshikawa, K., Sugimoto, A., Matsuo, N., Kabeya, N., Wang, L.,
1255 2003. Water Utilization of Natural and Planted Trees in the Semiarid Desert of
1256 Inner Mongolia , China Published by : Ecological Society of America WATER
1257 UTILIZATION OF NATURAL AND PLANTED TREES IN THE SEMIARID DESERT
1258 OF INNER MONGOLIA , CHINA. *Ecol. Appl.* 13, 337–351.
1259 Penna, D., Zanotelli, D., Scandellari, F., Aguzzoni, A., Engel, M., Tagliavini, M., Comiti,
1260 F., 2021. Water uptake of apple trees in the Alps: Where does irrigation water go?
1261 *Ecohydrology* 14, 1–16. <https://doi.org/10.1002/eco.2306>
1262 Plamboeck, A.H., Grip, H., Nygren, U., 1999. A hydrological tracer study of water
1263 uptake depth in a Scots pine forest under two different water regimes. *Oecologia*
1264 119, 452–460. <https://doi.org/10.1007/s004420050807>
1265 Prechsl, U.E., Burri, S., Gilgen, A.K., Kahmen, A., Buchmann, N., 2015. No shift to a
1266 deeper water uptake depth in response to summer drought of two lowland and
1267 sub-alpine C3-grasslands in Switzerland. *Oecologia* 177, 97–111.
1268 <https://doi.org/10.1007/s00442-014-3092-6>
1269 Ratajczak, Z., Nippert, J.B., Hartman, J.C., Ocheltree, T.W., 2011. Positive feedbacks
1270 amplify rates of woody encroachment in mesic tallgrass prairie. *Ecosphere* 2.
1271 <https://doi.org/10.1890/ES11-00212.1>
1272 Retzlaff, W.A., Blaisdell, G.K., Topa, M.A., 2001. Seasonal changes in water source of
1273 four families of loblolly pine (*Pinus taeda* L.). *Trees - Struct. Funct.* 15, 154–162.
1274 <https://doi.org/10.1007/s004680100087>
1275 Schulze, E.D., Mooney, H.A., Sala, O.E., Jobbagy, E., Buchmann, N., Bauer, G.,
1276 Canadell, J., Jackson, R.B., Loreti, J., Oesterheld, M., Ehleringer, J.R., 1996.
1277 Rooting depth, water availability, and vegetation cover along an aridity gradient in
1278 Patagonia. *Oecologia* 108, 503–511. <https://doi.org/10.1007/BF00333727>
1279 Sun, Q., Klaus, V.H., Wittwer, R., Liu, Y., Heijden, M.G.A. van der, Gilgen, A.K.,
1280 Buchmann, N., 2021. Water uptake patterns of pea and barley responded to
1281 drought but not to cropping systems. *Biogeosciences Discuss.* 1–37.
1282 <https://doi.org/10.5194/bg-2021-217>
1283 Wang, P., Song, X., Han, D., Zhang, Y., Liu, X., 2010. A study of root water uptake of
1284 crops indicated by hydrogen and oxygen stable isotope: A case in Shanxi

1285 Province, China. *Agric. Water Manag.* 97, 475–482.
1286 <https://doi.org/10.1080/10643389.2012.728825>
1287 Weltzin, J.F., McPherson, G.R., 1997. Spatial and temporal soil moisture resource
1288 partitioning by trees and grasses in a temperate savanna, Arizona, USA.
1289 *Oecologia* 112, 156–164. <https://doi.org/10.1007/s004420050295>
1290 Williams, D.G., Ehleringer, J.R., 2000. Intra- and interspecific variation for summer
1291 precipitation use in pinyon-juniper woodlands. *Ecol. Monogr.* 70, 517–537.
1292 [https://doi.org/10.1890/0012-9615\(2000\)070\[0517:IAIVFS\]2.0.CO;2](https://doi.org/10.1890/0012-9615(2000)070[0517:IAIVFS]2.0.CO;2)
1293 Wu, Y., Du, T., Li, F., Li, S., Ding, R., Tong, L., 2016. Quantification of maize water
1294 uptake from different layers and root zones under alternate furrow irrigation using
1295 stable oxygen isotope. *Agric. Water Manag.* 168, 35–44.
1296 <https://doi.org/10.1016/j.agwat.2016.01.013>
1297 Wu, Y., Zhou, H., Zheng, X.J., Li, Y., Tang, L.S., 2014. Seasonal changes in the water
1298 use strategies of three co-occurring desert shrubs. *Hydrol. Process.* 28, 6265–
1299 6275. <https://doi.org/10.1002/hyp.10114>
1300 Yang, B., Wen, X., Sun, X., 2015. Irrigation depth far exceeds water uptake depth in an
1301 oasis cropland in the middle reaches of Heihe River Basin. *Sci. Rep.* 5, 1–12.
1302 <https://doi.org/10.1038/srep15206>
1303 Zhu, Y., Jia, Z., Yang, X., 2011. Resource-dependent water use strategy of two desert
1304 shrubs on interdune, Northwest China. *J. Food, Agric. Environ.* 9, 832–835.
1305
1306